Table 8 Univariate and multivariate analysis of predictive factors for grade 3 or higher leukocytopenia throughout DEC

Factor		Category	Odds ratio	95% CI	*p*
Univariate analysis					
Age		Older than 68 versus younger than 68	1.111	0.262–4.719	0.886
MAP4	rs56313601	CT + TT versus CC	1.250	0.263–5.936	0.779
MAPT	rs3744460	CC versus CA + AA	2.139	0.472–9.699	0.458
ABCG2	rs2231137	AA versus AG + GG	1.071	0.061–18.82	0.962
CYP3A5	rs776746	*1/*3 + *1/*1 versus *3/*3	1.077	0.132–8.797	0.945
XRCC1-C194T	rs1799782	TT versus CC + CT	2.167	0.334–14.057	0.654
XRCC1-A399G	rs25487	GG versus GA + AA	2.514	0.581–10.882	0.285
ABCB1-C3435T	rs1045642	TT versus CC + CT	10.000	1.030–97.044	0.037
ABCB1-intron	rs7779562	GG versus GC + CC	1.905	0.454–7.983	0.479
Multivariate analysis					
Age		Older than 68 versus younger than 68	1.783	0.203–15.625	0.602
MAP4	rs56313601	CT + TT versus CC	1.082	0.133–8.783	0.941
MAPT	rs3744460	CC versus CA + AA	1.007	0.144–7.058	0.994
ABCG2	rs2231137	AA versus AG + GG	2.144	0.036–127.539	0.714
CYP3A5	rs776746	*1/*3 + *1/*1 versus *3/*3	1.083	0.067–17.458	0.955
XRCC1-C194T	rs1799782	TT versus CC + CT	4.247	0.172–105.138	0.377
XRCC1-A399G	rs25487	GG versus GA + AA	2.863	0.418–19.622	0.284
ABCB1-C3435T	rs1045642	TT versus CC + CT	32.141	1.253–824.316	0.036
ABCB1-intron	rs7779562	GG versus GC + CC	1.670	0.192–14.537	0.642

treated with DEC therapy. Thrombocytosis is known to be present in a wide range of malignancies, with a reported incidence of 10–57% [14]. Interestingly, Helley et al. [15] suggested that the level of platelet microparticles, which may affect tumour chemotaxins, adhesion and proliferation, was a potential prognostic factor in patients with CRPC undergoing docetaxel-based chemotherapy.

The individual variation in therapeutic effect may be due to the biological characteristics of the cancer itself and the innate properties of the patient as the cancer host. These variations are partially explained by genetic polymorphism, as represented by SNPs. Although the sample size was small, we found that the TT genotype of the *ABCB1* C3435T polymorphism was an independent predictor of severe leukocytopenia in patients with CRPC treated with DEC regimen. ABCB1 is responsible for a large portion of the systemic efflux capacity towards docetaxel. ABCB1 expression and protein folding are reported to be largely influenced by 3 SNPs including C3435T [16]. Sissung et al. [17] revealed that these variations correlated with survival, neutropenia and peripheral neuropathy in prostate cancer patients. Although further study is warranted to assess other *ABCB1* SNPs that are known to be associated with drug metabolism, our results support the view that the genotype of *ABCB1* SNPs has significant association with ARs induced by docetaxel-based chemotherapy.

In spite of limited sample size, the results of this phase II study evaluating DEC regimen showed that it has a high response rate and potential survival benefits in late-stage CRPC. We have demonstrated a significant impact of LDH levels on prediction of overall survival. Furthermore, the *ABCB1* C3455T polymorphism was associated with severe leukocytopenia, indicating that genotype analysis of the *ABCB1* polymorphism may be useful in predicting severe leukocytopenia in patients undergoing combination chemotherapy with DEC.

Acknowledgments We thank Yukiko Sugiyama and Yoko Mitobe for their excellent technical assistance.

Conflict of interest No author has any conflict of interest.

References

1. Jemal A, Siegel R, Ward E et al (2008) Cancer statistics, 2008. CA Cancer J Clin 58:71–96
2. Petrylak DP, Tangen CM, Hussain MH et al (2004) Docetaxel and estramustine compared with mitoxantrone and prednisone for advanced refractory prostate cancer. N Engl J Med 351: 1513–1520
3. Tannock IF, de Wit R, Berry WR et al (2004) Docetaxel plus prednisone or mitoxantrone plus prednisone for advanced prostate cancer. N Engl J Med 351:1502–1512
4. Regan MM, O'Donnell EK, Kelly WK et al (2010) Efficacy of carboplatin–taxane combinations in the management of castration-resistant prostate cancer: a pooled analysis of seven prospective clinical trials. Ann Oncol 21:312–318

5. Soga N, Kato M, Nishikawa K et al (2009) Intermittent docetaxel therapy with estramustine for hormone-refractory prostate cancer in Japanese patients. Int J Clin Oncol 14:130–135
6. Tsuchiya N, Wang L, Suzuki H et al (2006) Impact of IGF-I and CYP19 gene polymorphisms on the survival of patients with metastatic prostate cancer. J Clin Oncol 24:1982–1989
7. Tsuchiya N, Inoue T, Narita S et al (2008) Drug related genetic polymorphisms affecting adverse reactions to methotrexate, vinblastine, doxorubicin and cisplatin in patients with urothelial cancer. J Urol 180:2389–2395
8. Scher HI, Halabi S, Tannock I et al (2008) Design and end points of clinical trials for patients with progressive prostate cancer and castrate levels of testosterone: recommendations of the Prostate Cancer Clinical Trials Working Group. J Clin Oncol 26:1148–1159
9. Japanese Urological Association and the Japanese Society of Pathology (2001) General rule for clinical and pathological studies on prostatic cancer. Kanehara, Tokyo
10. Halabi S, Small EJ, Kantoff PW et al (2003) Prognostic model for predicting survival in men with hormone-refractory metastatic prostate cancer. J Clin Oncol 21:1232–1237
11. Halabi S, Vogelzang NJ, Kornblith AB et al (2008) Pain predicts overall survival in men with metastatic castration-refractory prostate cancer. J Clin Oncol 26:2544–2549
12. Kikuno N, Urakami S, Nakamura S et al (2007) Phase-II study of docetaxel, estramustine phosphate, and carboplatin in patients with hormone-refractory prostate cancer. Eur Urol 51:1252–1258
13. Beer TM, Ryan CW, Venner PM et al (2008) Intermittent chemotherapy in patients with metastatic androgen-independent prostate cancer: results from ASCENT, a double-blinded, randomized comparison of high-dose calcitriol plus docetaxel with placebo plus docetaxel. Cancer 112:326–330
14. Sierko E, Wojtukiewicz MZ (2004) Platelets and angiogenesis in malignancy. Semin Thromb Hemost 30:95–108
15. Helley D, Banu E, Bouziane A et al (2009) Platelet microparticles: a potential predictive factor of survival in hormone-refractory prostate cancer patients treated with docetaxel-based chemotherapy. Eur Urol 56:479–484
16. Kimchi-Sarfaty C, Oh JM, Kim IW et al (2007) A "silent" polymorphism in the MDR1 gene changes substrate specificity. Science 315:525–528
17. Sissung TM, Baum CE, Deeken J et al (2008) ABCB1 genetic variation influences the toxicity and clinical outcome of patients with androgen-independent prostate cancer treated with docetaxel. Clin Cancer Res 14:4543–4549

Translational Medicine

Yuasa et al. Translational Medic 2012, S:2
http://dx.doi.org/10.4172/2161-1025.S2-003

Review Article Open Access

Molecular Targeted Therapies for Patients with Metastatic Renal Cell Cancer

Takeshi Yuasa[1,2]*, Yasuhisa Fujii[1], Shunji Takahashi[2], Iwao Fukui[1] and Junji Yonese[1]

[1]*Department of Urology, Cancer Institute Hospital, Japanese Foundation for Cancer Research, Ariake, Tokyo, 135-8550, Japan*
[2]*Department of Medical Oncology, Cancer Institute Hospital, Japanese Foundation for Cancer Research, Ariake, Tokyo, 135-8550, Japan*

Abstract

Major breakthroughs have occurred recently in the knowledge of the genetics and transduction pathways involved in various malignancies, including renal cell cancer (RCC). Novel targeted therapies directed against angiogenesis and the mammalian target of rapamycin (mTOR) pathway is now being developed for the treatment of metastatic RCC. Currently, four anti-angiogenesis agents, (sorafenib, sunitinib, bevacizumab, pazopanib) and two specific inhibitors of the mTOR kinase (temsirolimus and everolimus) are approved by the United States Food and Drug Administration. Moreover, at least three other tyrosine kinase inhibitors (TKI) (axitinib from Pfizer, tivozanib from AVEO Pharmaceuticals, and dovitinib from Novartis) are in advanced stages of clinical trials. Here, we will discuss the molecular targeted agents for RCC patients in clinical trials as well as in clinical practice.

Introduction

Renal cell cancer (RCC) is the most frequently occurring solid lesion within the kidney, and its incidence is currently on the increase [1]. Radical nephrectomy remains the standard and only curative therapy for patients with localized RCC [2,3]. However, at initial diagnosis, one-third of RCC patients exhibit visceral metastasis, and up to half of the remainder eventually develop distant metastases [2,4]. Most RCCs have high levels of expression of the multidrug resistance protein P-glycoprotein and are therefore resistant to cytotoxic chemotherapies [2,4]. For a long time, the only effective therapeutic and preventive agents for distant metastases and local recurrence have been interferon (IFN) and interleukin (IL)-2, although these agents have achieved response rates of only 15% [2,3]. Recently, major breakthroughs have occurred in the knowledge of the genetics and transduction pathways involved in various malignancies, including RCC [5]. Novel targeted therapies directed against angiogenesis and the mammalian targets of rapamycin (mTOR) pathway are now being developed for the treatment of metastatic RCC. At the moment, the United States Food and Drug Administration (FDA) has approved four anti-angiogenesis agents: sorafenib (Nexavar; Bayer) [6], sunitinib (Sutent; Pfizer) [7], bevacizumab (Avastin; Genentech/Roche) [8], and pazopanib (Votrient; GlaxoSmithKline) [9]. The FDA has also approved two specific inhibitors of the mTOR kinase, temsirolimus (Torisel; Pfizer) [10] and everolimus (Afinitor; Novartis) [11]. Moreover, at least three other tyrosine kinase inhibitors (TKI) (Axitinib Pfizer; Tivozanib, AVEO Pharmaceuticals; and Dovitinib, Novartis) have reached advanced stages of clinical trials [12]. Here, we describe the molecular targeted agents for RCC patients in clinical trials as well as in clinical practice.

Approved molecular targeted agents and their clinical trials

At first, we describe the clinical efficacy of the six agents currently approved by the FDA. These include four anti-angiogenesis agents, among which sorafenib, sunitinib, and pazopanib are TKI, whereas bevacizumab is a humanized monoclonal antibody that inhibits VEGF-A. The two mTOR inhibitors are temsirolimus and everolimus. The clinical studies mentioned here are summarized in Table 1.

Sorafenib: Sorafenib, an orally active multikinase inhibitor, targets Raf kinase protein; VEGF receptors (VEGFR)-1, 2, and 3; platelet-derived growth factor receptor β (PDGFR-β); FMS-like tyrosine kinase 3 (Flt-3); c-Kit protein (c-Kit); and RET receptor tyrosine kinases [6]. Sorafenib is the first molecular agent targeted at metastatic RCC, demonstrating prolonged progression-free survival (PFS) compared with placebo in patients with advanced cytokine-refractory RCC (n=903) in the phase III clinical study known as Treatment Approaches in Renal Cancer Global Evaluation Trial (TARGET) [6]. In TARGET, the median PFS was significantly longer (5.5 months) in the sorafenib group than in the placebo group (2.8 month) [6]. Partial responses were reported as the best response in 10% of patients receiving sorafenib and in 2% of those receiving placebo ($P<0.001$) [6]. The final overall survival (OS) of patients receiving sorafenib was comparable with that of patients receiving placebo (17.8 v 15.2 months, $P=0.146$); however, when post-cross-over placebo survival data were censored, the difference became significant (17.8 v 14.3 months, respectively; $P=0.029$) [13]. Diarrhea, rash, fatigue, and hand-foot syndrome (HFS) were the most common adverse events (AE) associated with sorafenib [6]. These AEs are commonly mild and easily manageable as compared with standard chemotherapies. However, as we reported previously, sorafenib-associated erythema multiforme, which is a toxic mucocutaneous disease with significant morbidity and mortality, might not be a rare AE in Japanese patients [14]. In addition, from a recent phase II dose escalation study of sorafenib, a half of patients (3/6) could be benefitted with PFS of more than 3 months from the escalated dose (600 mg twice a day) due to early progression [15].

Sunitinib: Sunitinib, which is the best available in the United States (Research from the Synovate Healthcare US Tandem Oncology Monitor 2007–2010) for patients with RCC, is an orally administered multi-targeted tyrosine kinase inhibitor [5]. The main targets of sunitinib are VEGF receptors-1-3 and PDGFRs-α and -β [7]. A randomized multicenter phase III trial was conducted enrolling 750 patients with treatment-naive, metastatic RCC to receive either

***Corresponding author:** Takeshi Yuasa, Department of Urology and Medical Oncology, Cancer Institute Hospital, Japanese Foundation for Cancer Research, Tokyo, 138-8550, Japan, Tel: 81-3-3520-0111; Fax: 81-3570-0343; E-mail: takeshi.yuasa@jfcr.or.jp

Received January 25, 2012; **Accepted** February 01, 2012; **Published** February 03, 2012

Citation: Yuasa T, Fujii Y, Takahashi S, Fukui I, Yonese J (2012) Molecular Targeted Therapies for Patients with Metastatic Renal Cell Cancer. Translational Medic S2:003. doi:10.4172/2161-1025.S2-003

Agent	Patients	Number	Control	PFS (months)	probability	OS (months)	probability	US-FDA approval	References
sorafenib	cytokine refractory	903	placebo	5.5 vs 2.8	<0.01	17.8 vs 15.2	0.146	approved	6, 15
sunitinib	treatment naïve	750	interferon	11 vs 5	<0.001	26.4 vs 21.8	0.051	approved	7, 17
bevacizumab	treatment naïve treatment naïve or cytokine	649	interferon	10.2 vs 5.4	0.0001	23.3 vs 21.3	0.336	approved	8, 18
pazopanib	refractory	435	placebo	9.2 vs 4.2	<0.001	ND		approved	9
temsirolimus	treatment naïve	625	interferon	3.8 vs 1.9	<0.001	10.9 vs 7.3	0.008	approved	10
everolimus	TKI refractory	410	placebo	4.0 vs 1.9	<0.0001	14.8 vs 14.4	0.162	approved	11,19
axitinib	cytokine or TKI refractory treatment naïve or cytokine	723	sorafenib	6.7 vs 4.7	<0.0001	ND		approved	22
tivozanib	refractory		sorafenib	ND		ND		not yet	24
dovitinib	TKI and mTOR refractory		sorafenib	ND		ND		not yet	

PFS: median progression free survival (agents versus control), OS: median overall survival (agents versus control), US-FDA: the United States Food and Drug Administration, TKI: tyrosine kinase inhibitor, mTOR: mammalian target of rapamycin

Table 1: Summary of the results of phase III clinical trials of molecular targeted agents for patients with metastatic renal cell cancer.

repeated 6-week cycles of sunitinib (at a dose of 50 mg given orally once daily for 4 weeks, followed by 2 weeks without treatment) or IFN-α (at a dose of 9 MU given subcutaneously three times weekly) [7]. Median PFS was 11 months for sunitinib compared with 5 months for IFN-α ($P = 0.001$) [7]. As cross-over was allowed in this study, the final report showed that median OS tended to be longer in the sunitinib group than in the IFN-α group (26.4 *vs* 21.8 months, respectively, $P = 0.051$) [16]. The objective response rate was 47% for sunitinib compared with 12% for IFN-α ($P = 0.001$) [7,16]. In addition, an exploratory analysis, which censored the 25 patients from the IFN-α group who had crossed over to receive sunitinib, showed a median overall survival time of 26.4 months for the sunitinib group compared with 20.0 months for the IFN-α group ($P = 0.036$) [16]. The AEs were controllable, with the most commonly reported sunitinib-related grade 3 AEs being hypertension (12%), fatigue (11%), diarrhea (9%), and HFS (9%) [7,16].

Bevacizumab: Bevacizumab is a humanized monoclonal antibody that inhibits VEGF. In Europe, a multicenter, randomized, double-blind, phase III trial was conducted of the combination of bevacizumab and IFN-α compared with IFN-α alone for 649 metastatic RCC patients [8]. Median duration of PFS was significantly longer in the bevacizumab plus IFN-α group than that in IFN alone (10.2 months *vs* 5.4 months, $P=0.0001$). Increases in PFS were seen with bevacizumab plus IFN-α, irrespective of risk group or whether reduced-dose IFN-α was received [8]. However, median OS was not significantly different (23.3 months with bevacizumab plus IFN and 21.3 months with IFN plus placebo). The authors commented that patients (> 55%) in both arms received at least one post-protocol anti-neoplastic therapy, possibly confounding the OS analysis [17]. The most commonly reported grade 3 or worse AEs were fatigue (40 [12%] patients in the bevacizumab group *vs* 25 [8%] in the IFN-alone group) and asthenia (34 [10%] *vs*20 [7%]) [8].

Pazopanib: Pazopanib is a second-generation oral angiogenesis inhibitor targeting VEGFRs-1-3, PDGFRs-α and β, and c-Kit [9]. An international randomized, double-blind, placebo-controlled phase III study evaluated the efficacy and safety of pazopanib in treatment-naive and cytokine-pretreated patients with metastatic RCC (n=435) [9]. PFS was significantly prolonged with pazopanib compared with placebo in the overall study population (median, PFS 9.2 v 4.2 months, $P<0.0001$), the treatment-naive subpopulation (median PFS 11.1 v 2.8 months, $P<0.0001$), and the Cytokine-pretreated subpopulation (median PFS, 7.4 v 4.2 months, $P<0.001$) [9]. The objective response rate was 30% with pazopanib compared with 3% with placebo ($P<0.001$) [9]. It is remarkable that no clinically important differences in quality of life were reported for pazopanib versus placebo [9]. Due to these efficacy and safety profiles, the FDA approved pazopanib in 2009, the sixth molecular targeted drug to be approved for metastatic RCC. Currently, an international randomized, phase III study is underway to evaluate the efficacy and safety of pazopanib compared with sunitinib in treatment-naive patients with metastatic RCC.

Temsirolimus: mTOR is a serine/threonine protein kinase that regulates cell growth, cell proliferation, and cell motility. mTOR belongs to the phosphatidylinositol 3-kinase-related kinase protein family and play important roles in survival and growth of cancer cells; thus, it is considered to be a target of molecular targeted agents. Temsirolimus is an intravenously administered mTOR inhibitor. A multicenter, randomized, phase III clinical trial was conducted for 626 patients with previously untreated, poor-prognosis metastatic RCC [10]. In this trial, median overall survival times in the IFN group, the temsirolimus group, and the IFN and temsirolimus combination-therapy group were 7.3, 10.9, and 8.4 months, respectively [10]. The patients who received temsirolimus alone had longer OS ($P = 0.008$) and PFS ($P<0.001$) than did patients who received IFN alone [10]. Rash, peripheral edema, hyperglycemia, and hyperlipidemia were more common in the temsirolimus group, but there were still fewer patients with serious AEs in the temsirolimus group than in the IFN group ($P=0.02$) [10]. In this study, interstitial lung disease was found to be a rare AE [10]. However, nowadays in clinical practice, interstitial lung disease is the most serious AE for the agents of this category, which includes temsirolimus and everolimus.

Everolimus: Everolimus is another oral-administered mTOR inhibitor. The RECORD-1 (*Re*nal *C*ell cancer treatment with *O*ral *RAD*001 given *D*aily) trial was an international phase III, randomized, double-blind, placebo-controlled trial in patients with metastatic RCC (n=410) whose disease had progressed on VEGF-targeted therapy [11]. In this study, a significant difference in efficacy was observed between arms, and the trial was halted early after 191 progression events had occurred (median PFS 4.0 for the everolimus group *vs* 1.9 months for the placebo group, $P<0.0001$) [11]. As 80% of patients in the placebo arm crossed over to everolimus, the median OS differed very little, 14.8 months (everolimus) versus 14.4 months (placebo) ($P=0.162$) [18]. Although stomatitis and rash were the most commonly reported AEs, they were mostly mild or moderate. Interstitial lung disease was the most important AE, detected in 22 (8%) patients in the everolimus group, of whom eight had pneumonitis of grade 3 severity [11]. Everolimus is the first agent to show significant benefit for metastatic RCC patients

after approved targeted therapies such as sunitinib and sorafenib have failed. In addition, currently, treatment of mTOR inhibitor-refractory remains largely undefined. Recently, Grunwald reported on 40 patients who received sunitinib (n=19), sorafenib (n=8), dovitinib (n=10) or Bevacizumab/interferon (n=3) after failure of everolimus. Median PFS, OS, and RR were 5.5 months (range 0.4–22.3) 11.3 months (range 0.8–22.3) and 10% (n=4). From their results, anti-angiogenesis agents might be attractive in everolimus-resistant metastatic RCC [19].

Investigating new drugs

In this section, we report recent advances in the development of second-generation VEGFR TKIs, axitinib, tivozatinib, linifanib, and dovitinb, focusing on their potential benefits of improved potency and selectivity. The former three agents are potent selective inhibitor of VEGFR, whereas the latter targets not only VEGFRs but also Fibroblast growth factor receptor (FGFR).

Axitinib: Axitinib is an oral, potent, and highly selective tyrosine kinase inhibitor among the known VEGFRs, with lower potency against PDGFR and c-kit [20]. In an initial phase II clinical trial for 52 patients with cytokine-refractory metastatic RCC, axitinib demonstrated clinical activity with two complete and 21 partial responses (objective response rate (ORR): 44.2%, 95% CI 30.5-58.7) [20]. In addition, 22 patients showed SD for longer than 8 weeks, including 13 patients with stable disease for 24 weeks or longer [20]. Median PFS was 15.7 months (8.4-23.4, range 0.03-31.5) and median OS was 29.9 months (20.3-not estimable; range 2.4-35.8) [19]. Although 28 patients had grade 3 or grade 4 treatment-related AEs, these AEs were generally manageable and controlled by dose modification or supportive care, or both [20]. After the hopeful results of the phase II clinical trial for patients with sorafenib-refractory metastatic RCC [21], a randomized, open-label, phase III trial compared the efficacy and safety of axitinib versus sorafenib as second-line therapy for metastatic RCC. In this study, 723 patients were randomized to either axitinib (n=361) or sorafenib (n=362), with axitinib demonstrating a significantly longer PFS (medianPFS: 6.7 months for axitinib vs 4.7 months for sorafenib, $P<0.0001$) and higher objective response rate (19.4% for axitinib vs 9.4% for sorafenib, $P=0.0001$) with an acceptable safety profile [22]. In a recent Japanese phase II study of axitinib for the patients with cytokine-refractory metastatic RCC, axitinib also demonstrated significant efficacy for metastatic RCC and was well tolerated in this population. In addition, preliminary findings from this population suggested that baseline proteinuria and soluble VEGFR-2 levels might be key indicators for axitinib-induced proteinuria and efficacy, respectively [23]. To obtain approval as the seventh agent for metastatic RCC, axitinib has been submitted to the FDA and the Japanese Ministry of Health, Labour and Welfare.

Tivozanib: Tivozanib is a potent selective inhibitor of VEGFR-1, 2, and 3 kinases (IC50 0.21, 0.16 and 0.24 nM respectively), and inhibits c-Kit and PDGFR at 10 times higher concentrations (IC50 1.63 and 1.72 nM respectively) [24]. In a phase II randomized clinical trial of tivozanib (1.5 mg/day; 3 weeks on, 1 week off) in patients with metastatic RCC, 272 patients were enrolled, among whom 53% were treatment naïve, 72% had undergone nephrectomy, and 83% had RCC with a clear cell component [24]. The ORR (complete response [CR] +PR) was 27.2%, SD 60.5% and disease control rate (CR/PR + SD) 87.7%. The most common treatment-related AEs (all grades) were hypertension (42%) and dysphonia (16%) [23]. In this phase II clinical trial, tivozanib was active in RCC, and the AE profile of this agent was consistent with that of a selective VEGFR inhibitor, with minimal off-target toxicities. Based on this favorable antitumor activity and safety profile, a phase III, randomized, controlled global, multicenter trial is currently in progress to compare tivozanib with sorafenib in patients with advanced RCC [25]. In addition, based on the selective VEGFR inhibition and the minimal off-target toxicities, a combination phase I clinical trial of tivozanib and temsirolimus was conducted [26]. Preliminary results indicated that the combination of tivozanib with temsirolimus was well tolerated and showed clinical activity in patients with advanced RCC [26]. The investigators concluded that tivozanib was the first VEGFR TKI that could be combined with temsirolimus at the full dose and schedule of both agents [26].

Linifanib: Linifanib (ABT-869, Abbott Laboratories) is a novel anti-angiogenesis agent, selective for all VEGFR and PDGFR with minimal activity against unrelated receptor tyrosine kinases, cytosolic tyrosine kinases and serine/threonine kinases [27]. The open-label, multicentre, phase II trial of oral linifanib was conducted for the patients with advanced RCC (n=43) who were previously treated with sunitinib. ORR was 13.2% and median PFS and OS were 5.4 months and 14.5 months, respectively [28]. The most common treatment-related AEs were diarrhea (74%), fatigue (74%) and hypertension (66%), and the most common treatment-related Grade 3/4 AE was hypertension (40%) [28]. The investigators concluded that linifanib demonstrated clinically meaningful activity in patients with advanced RCC after sunitinib failure and further investigation is necessary [28].

Dovitinib: Dovitinib is a potent receptor TKI that selectively targets VEGFR, PDGFR, FGFR, c-KIT, RET, and Flt-3. Compared to other TKI agents, dovitinib additionally targets FGFR, whose mediated signal has been reported to be an important escape mechanism of anti-VEGFR therapies [29]. In an early phase I study, maximum tolerated dose (MTD) of dovitinib, which was administered p.o. on a 5-day on/2-day off schedule in a repeated 28-day cycle, was defined as 500 mg/day [29]. In a phase II clinical trial for patients with clear cell metastatic RCC, in patients previously treated with a VEGFR inhibitor and mTOR inhibitor (n=31), the best ORRs per central review included PR, 3 (10%); SD more than 4 months, 13 (42%); PD, 6 (19%); and unknown/not assessed, 4 (13%) [30]. Median PFS and OS in these patients were 6.1 and 10.2 months for this group, respectively [30]. Dovitinib demonstrated encouraging antitumor activity with a well-tolerated safety profile in patients with heavily pretreated metastatic RCC [30]. Based on this favorable profile, a phase III, randomized, controlled, global, multicenter trial is currently in progress to compare dovitinib with sorafenib in patients with RCC previously treated with a VEGFR inhibitor and mTOR inhibitor.

Biomarkers to predict response to targeted therapy and prognosis in metastatic RCC

We previously provided a brief overview of biomarkers for

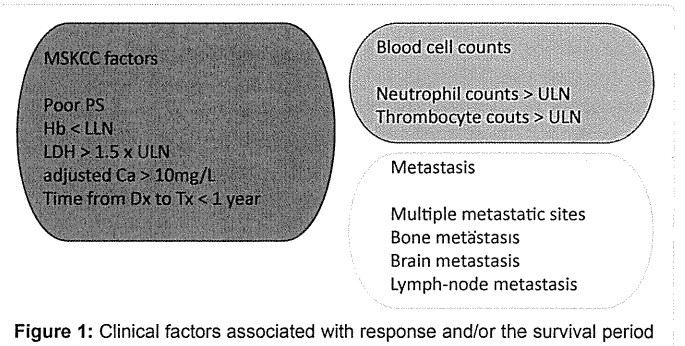

Figure 1: Clinical factors associated with response and/or the survival period of the renal cell cancer patients treated with the targeted agents.

sunitinib and the other targeted agents used in the treatment of metastatic RCC [5]. Regarding clinical factors, the MSKCC prognostic factors, named after the Memorial Sloan Kettering Cancer Center in the cytokine era, include low Karnofsky performance status (PS), high lactate dehydrogenase (LDH), low hemoglobin (Hb), high corrected serum calcium (Ca), and time from initial RCC diagnosis to start of systemic therapy of less than one year, seem to be valid predictors of survival in metastatic RCC [31,32]. In addition to the factors included in the MSKCC score, the number of neutrophils, the platelet count, and the number and/or location of metastatic lesions might be independent prognostic factors in patients treated with molecular targeted agents (Figure 1) [33-35]. The clinical efficacy of sunitinib depends on the systemic exposure of the targeted organ to the active compounds. Orally administered sunitinib is absorbed by the intestinal mucosa and metabolized in the liver. The ATP-binding cassette (ABC) transporter proteins, particularly multidrug resistance 1 [MDR1/ATP binding cassette member B1 (ABCB1), formerly known as P-glycoprotein (P-gp)] and breast cancer resistance protein [BCRP/ATP binding cassette member G2, formerly known as mitoxantrone resistant protein (MXR)], mediate absorption and/or excretion through the intestinal wall and regulate the efflux of a wide variety of anticancer drugs from target cells. These efflux transporter proteins and the cytochrome P450 3A (CYP3A) family play a role in the absorption and metabolism of the agents, respectively [5,36]. The active metabolite and the parent sagents are multi-targeted TKIs that inhibit PDGFR-α and -β; VEGFR-1, -2 and -3; stem cell factor receptor c-Kit; Flt-3 [5,37]. Very recently, Spanish Oncology Genitourinary Group's observational and prospective study demonstrated that two *VEGFR3* missense polymorphisms were associated with reduced PFS with sunitinib and a *CYP3A5*1* high metabolising allele was associated with an increased risk of dose reductions due to toxicity [38]. The efficacy of TKIs can be influenced by multiple genes encoding efflux transporters, metabolizing enzymes, and targeted tyrosine kinases [38-41]. The known adverse effects of the targeted agents include HFS, diarrhea, stomatitis, hypertension, fatigue and hypothyroidism. If AEs depend on the degree of systemic exposure to sunitinib, on which clinical efficacy also depends, AEs may be potential predictors of sunitinib efficacy in metastatic RCC patients. Indeed, these correlations have been reported between clinical response and hypertension, hypothyroidism, and HFS [5,42-44].

Conclusion

In this review, we discussed the approved targeted agents for patients with metastatic RCC and the second-generation targeted agents currently in development. In addition, we briefly reviewed currently reported biomarkers. These targeted agents have been and will likely continue to be used widely for the treatment of RCC. However, several crucial questions remain unanswered. Is any combination of the targeted agents possibly beneficial for patients? How best should these agents be sequenced? Currently we have no answer to either question. We hope that the survival period of patients with metastatic RCC can be prolonged, with a satisfactory quality of life, if we understand how to make optimal use of these targeted agents. We believe that this is our purpose and our mission. Further basic research as well as clinical studies is necessary to reach our goal.

Acknowledgments

This work was partly supported by the Takeda Science Foundation and Grants-in-Aid for Scientific Research from the Ministry of Education, Culture, Sports, Science and Technology, Japan.

References

1. Jemal A, Siegel R, Ward E, Hao Y, Xu J, et al. (2009) Cancer statistics, 2009. CA Cancer J Clin 59: 225-249.
2. Campbell SC, Novick AC, Bukowski RM (2007) Renal tumors. In: Kavoussi LR, Novick AC, Partin AW, Peters CA, Wein AJ, eds. Campbell-Walsh Urology. (9th edn), New York: Saunders, 1567-1637.
3. Ljungberg B, Hanbury DC, Kuczyk MA, Merseburger AS, Mulders PF, et al. (2007) European Association of Urology Guideline Group for renal cell carcinoma. Renal cell carcinoma guideline. Eur Urol 51: 1502-1510.
4. Linehan WM, Vasselli J, Srinivasan R, Walther MM, Merino M, et al. (2004) Genetic basis of cancer of the kidney: disease-specific approaches to therapy. Clin Cancer Res 10: 6282S-6289S.
5. Yuasa T, Takahashi S, Hatake K, Yonese J, Fukui I (2011) Biomarkers to Predict Response to Sunitinib Therapy and Prognosis in Metastatic Renal Cell Cancer. Cancer Science 102: 1949-1957.
6. Escudier B, Eisen T, Stadler WM, Szczylik C, Oudard S, et al. (2007) TARGET Study Group. Sorafenib in advanced clear-cell renal-cell carcinoma. N Engl J Med 356: 125-134.
7. Motzer RJ, Hutson TE, Tomczak P, Michaelson MD, Bukowski RM, et al. (2007) Sunitinib versus interferon alfa in metastatic renal cell carcinoma. N Engl J Med 356: 115-124.
8. Escudier B, Pluzanska A, Koralewski P, Ravaud A, Bracarda S, et al. (2007) AVOREN Trial investigators. Bevacizumab plus interferon alfa-2a for treatment of metastatic renal cell carcinoma: a randomised, double-blindphase III trial. Lancet 370: 2103-2111.
9. Hutson TE, Davis ID, Machiels JP, De Souza PL, Rottey S, et al. (2010) Efficacy and safety of pazopanib in patients with metastatic renal cell carcinoma. J Clin Oncol 28: 475-480.
10. Hudes G, Carducci M, Tomczak P, Dutcher J, Figlin R, et al. (2007) Global ARCC Trial. Temsirolimus, interferon alfa, or both for advanced renal-cell carcinoma. N Engl J Med 356: 2271-2281.
11. Motzer RJ, Escudier B, Oudard S, Hutson TE, Porta C, et al. (2008) RECORD-1 Study Group. Efficacy of everolimus in advanced renal cell carcinoma: a double-blind, randomised, placebo-controlled phase III trial. Lancet 372: 449-456.
12. Heng DY, Kollmannsberger C, Chi KN (2010) Targeted therapy for metastatic renal cell carcinoma: current treatment and future directions. Ther Adv Med Oncol 2: 39-49.
13. Escudier B, Eisen T, Stadler WM, Szczylik C, Oudard S, et al. (2009) Sorafenib for treatment of renal cell carcinoma: Final efficacy and safety results of the phase III treatment approaches in renal cancer global evaluation trial. J Clin Oncol 27: 3312-3318.
14. Kodaira M, Takahashi S, Takeuchi K, Yuasa T, Saotome T, et al. (2010) Erythema multiforme induced by sorafenib for metastatic renal cell carcinoma in Japanese patients. Ann Oncol 21: 1563-1565.
15. Mancuso A, Di Paola ED, Leone A, Catalano A, Calabrò F, et al. (2012) Phase-II escalation study of sorafenib in patients with metastatic renal cell carcinoma who have been previously treated with anti-angiogenic treatment. BJU Int 109: 200-206.
16. Motzer RJ, Hutson TE, Tomczak P, Michaelson MD, Bukowski RM, et al. (2009) Overall survival and updated results for sunitinib compared with interferon alfa in patients with metastatic renal cell carcinoma. J Clin Oncol 27: 3584-3590.
17. Escudier B, Bellmunt J, Négrier S, Bajetta E, Melichar B, et al. (2010) Phase-III trial of bevacizumab plus interferon alfa-2a in patients with metastatic renal cell carcinoma (AVOREN): final analysis of overall survival. J ClinOncol 28: 2144-2150.
18. Motzer RJ, Escudier B, Oudard S, Hutson TE, Porta C, et al. (2010) RECORD 1Study Group. Phase 3 trial of everolimus for metastatic renal cell carcinoma: final results and analysis of prognostic factors. Cancer 116: 4256-4265.
19. Grünwald V, Seidel C, Fenner M, Ganser A, Busch J, et al. (2011) Treatment of everolimus-resistant metastatic renal cell carcinoma with VEGF-targeted therapies. Br J Cancer 105: 1635-1639.
20. Rixe O, Bukowski RM, Michaelson MD, Wilding G, Hudes GR, et al. (2007) Axitinib treatment in patients with cytokine-refractory metastatic renal-cell cancer: a phase II study. Lancet Oncol 8: 975–984.
21. Rini BI, Wilding G, Hudes G, Wilding G, Hudes GR, et al. (2009) Phase-II study of axitinib in sorafenib-refractory metastatic renal cell carcinoma. J Clin Oncol 27: 4462–4468.
22. Rini BI, Escudier B, Tomczak P, Kaprin A, Szczylik C, et al. (2011) Comparative effectiveness of axitinib versus sorafenib in advanced renal cell carcinoma (AXIS): a randomised phase 3 trial. Lancet 378: 1931-1939.

23. Tomita Y, Uemura H, Fujimoto H, Kanayama HO, Shinohara N, et al. (2011) Japans Axitinib Phase II Study Group. Key predictive factors of axitinib (AG-013736)-induced proteinuria and efficacy: a phase II study in Japanese patients with cytokine-refractory metastatic renal cell carcinoma. Eur J Cancer 47: 2592-2602.

24. Bhargava P, Esteves B, Nosov DO, Lipatov N, Lyulko AA, et al. (2009) Updated activity and safety results of a phase II randomized discontinuation trial (RDT) of AV-951, a potent and selective VEGFR1, 2, and 3 kinase inhibitor, in patients with renal cell carcinoma (RCC). Journal of Clinical Oncology 27: 5032.

25. Motzer RJ, Bhargava P, Esteves B, Al-Adhami M, Slichenmyer W, et al. (2011) A phase III, randomized, controlled study to compare tivozanib with sorafenibin patien ts (pts) with advanced renal cell carcinoma (RCC). J Clin Oncol 29.

26. Kabbinavar FF, Srinivas S, Hauke RJ, Amato RJ, Esteves B, et al. (2011) A phase I trial of combined tivozanib (AV-951) and temsirolimus therapy inpatients (pts) with renal cell carcinoma (RCC). J Clin Oncol 029.

27. Zhou J, Pan M, Xie Z, Loh SL, Bi C, et al. (2008) Synergistic antileukemic effects between ABT-869 and chemotherapy involve down regulation of cell cycle-regulated genes and c-Mos-mediated MAPK pathway. Leukemia 22: 138-1346.

28. Tannir NM, Wong YN, Kollmannsberger CK, Ernstoff MS, Perry DJ, et al. (2011) Phase 2 trial of linifanib (ABT-869) in patients with advanced renal cell cancer after sunitinib failure. Eur J Cancer 47: 2706-2714.

29. Angevin E, Lin C, Pande AU, Lopez JA, Gschwend J, et al. (2010) A phase I/ IIstudy of dovitinib (TKI258), a FGFR and VEGFR inhibitor, in patients (pts)with advanced or metastatic renal cell cancer: Phase I results. Journal of Clinical Oncology 28: 3057.

30. Angevin E, Grünwald V, Ravaud A, Castellano DE, Lin CC, et al. (2011) A phase II study of dovitinib (TKI258), an FGFR- and VEGFR-inhibitor, in patients with advanced or metastatic renal cell cancer (mRCC). J Clin Oncol 29.

31. Motzer RJ, Bacik J, Murphy BA, Russo P, Mazumdar M (2001) Interferon-alfa as a comparative treatment for clinical trials of new therapies against advanced renal cell carcinoma. J Clin Oncol 20: 289-296.

32. Yuasa T, Tsuchiya N, Urakami S, Horikawa Y, Narita S, et al. (2011) Clinical Efficacy and Prognostic Factors for Overall Survival in Japanese Patients with Metastatic Renal Cell Cancer Treated with Sunitinib. BJU int.

33. Heng DY, Xie W, Regan MM, Warren MA, Golshayan AR, et al. (2009) Prognostic factors for overall survival in patients with metastatic renal cell carcinoma treated with vascular endothelial growth factor-targeted agents: results from a large, multicenter study. J Clin Oncol 27: 5794-5799.

34. Choueiri TK, Garcia JA, Elson P, Khasawneh M, Usman S, et al. (2007) Clinical factors associated with outcome in patients with metastatic clear-cell renal cell carcinoma treated with vascular endothelial growth factor-targeted therapy. Cancer 110: 543-550.

35. Patil S, Figlin RA, Hutson TE, Michaelson MD, Négrier S, et al. (2011) Prognostic factors for progression-free and overall survival with sunitinib targeted therapy and with cytokine as first-line therapy in patients with metastatic renal cell carcinoma. Ann Oncol 22: 295-300.

36. Tsuchiya N, Satoh S, Tada H, Li Z, Ohyama C, et al. (2004) Influence of CYP3A5 and MDR1 (ABCB1) polymorphisms on the pharmacokinetics of tacrolimus in renal transplant recipients. Transplantation 78: 1182-1187.

37. Faivre S, Delbaldo C, Vera K, Robert C, Lozahic S, et al. (2006) Safety, pharmacokinetic and antitumor activity of SU11248, a novel oral multi target tyrosine kinase inhibitor, in patients with cancer. J Clin Oncol 24: 25-35.

38. Garcia-Donas J, Esteban E, Leandro-García LJ, Castellano DE, del Alba AG, et al. (2011) Single nucleotide polymorphism associations with response and toxic effects in patients with advanced renal-cell carcinoma treated with first-line sunitinib: a multicentre, observational, prospective study. Lancet Oncol 12: 1143-1150.

39. van Erp NP, Eechoute K, van der Veldt AA, Haanen JB, Reyners AK, et al. (2009) Pharmacogenetic pathway analysis for determination of sunitinib-induced toxicity. J Clin Oncol 27: 4406-4412.

40. van der Veldt AA, Eechoute K, Gelderblom H, Gietema J, Guchelaar HJ, et al.(2011) Genetic polymorphisms associated with a prolonged progression-free survival in patients with metastatic renal cell cancer treated with sunitinib. Clin Cancer Res 17: 620-629.

41. Xu CF, Bing NX, Ball HA, Rajagopalan D, Sternberg CN, et al. (2011) Pazopanib efficacy in renal cell carcinoma: evidence for predictive genetic markers in angiogenesis-related and exposure-related genes. J Clin Oncol 29: 2557-2564.

42. Rixe O, Billemont B, Izzedine H (2007) Hypertension as a predictive factor of Sunitinib activity. Ann Oncol 18: 1117.

43. Schmidinger M, Vogl UM, Bojic M, Lamm W, Heinzl H, et al. (2011) Hypothyroidism in patients with renal cell carcinoma: blessing or curse? Cancer 117:534-544.

44. Michaelson MD, Cohen DP, Li S, Motzer RJ, Escudier B, et al. (2011) Hand–Foot Syndrome as a Potential Biomarker of Efficacy in Patients with Metastatic Renal Cell Carcinoma Treated with Sunitinib. American Society of Clinical Oncology-Genito-Urinary oncology.

This article was originally published in a special issue, Clinical Studies of Molecular Targeted Therapies handled by Editor(s). Dr. Junya Kuroda, Kyoto Prefectural University of Medicine, Japan

Citation: Blood Cancer Journal (2011) 1, e15; doi:10.1038/bcj.2011.11

www.nature.com/bcj

ORIGINAL ARTICLE

The identification of irreversible rituximab-resistant lymphoma caused by *CD20* gene mutations

Y Mishima[1,2], Y Terui[1], K Takeuchi[3], Y Matsumoto-Mishima[1], S Matsusaka[1], R Utsubo-Kuniyoshi[1,2] and K Hatake[1]

[1]*Department of Clinical Chemotherapy, Cancer Chemotherapy Center, Japanese Foundation for Cancer Research, Tokyo, Japan;* [2]*Olympas Bio-Imaging Lab, Cancer Chemotherapy Center, Japanese Foundation for Cancer Research, Tokyo, Japan and* [3]*Division of Pathology, Cancer Institute, Japanese Foundation for Cancer Research, Tokyo, Japan*

C-terminal mutations of CD20 constitute part of the mechanisms that resist rituximab therapy. Most CD20 having a C-terminal mutation was not recognized by L26 antibody. As the exact epitope of L26 has not been determined, expression and localization of mutated CD20 have not been completely elucidated. In this study, we revealed that the binding site of L26 monoclonal antibody is located in the C-terminal cytoplasmic region of CD20 molecule, which was often lost in mutated CD20 molecules. This indicates that it is difficult to distinguish the mutation of CD20 from under expression of the CD20 protein. To detect comprehensive CD20 molecules including the resistant mutants, we developed a novel monoclonal antibody that recognizes the N-terminal cytoplasm region of CD20 molecule. We screened L26-negative cases with our antibody and found several mutations. A rituximab-binding analysis using the cryopreserved specimen that mutation was identified in CD20 molecules indicated that the C-terminal region of CD20 undertakes a critical role in presentation of the large loop in which the rituximab-binding site locates. Thus, combination of antibodies of two kinds of epitope permits the identification of C-terminal CD20 mutations associated with irreversible resistance to rituximab and may help the decision of the treatment strategy.
Blood Cancer Journal (2011) **1,** e15; doi:10.1038/bcj.2011.11; published online 8 April 2011
Keywords: B-cell lymphomas; mutations; antibody therapy; CD20; rituximab

Introduction

Previously, we reported that gene mutations of *CD20* were somehow involved in resistance to rituximab therapy, and we proposed that C-terminal deletion mutations of CD20 might be related to relapse/resistance after rituximab therapy.[1] Many of these C-terminal truncated CD20 molecules were not recognized by the L26 monoclonal antibody used routinely in most clinical laboratories. Therefore, expression of CD20 seemed to have been completely lost for these lymphomas. However, an immunohistochemical study using a polyclonal antibody showed that some kind of C-terminal truncated CD20 was present in cytoplasm, so it was possible that the epitope of L26 was lost by gene mutations.[1] L26 recognizes the cytoplasmic region of CD20 molecules, but no more detailed information about its epitope had been reported.[2,3] In this study, we determine a recognition site of L26 by using a series of deletion mutants of CD20 molecules. In addition, to detect every one of the mutated CD20 molecules, we developed new antibodies that recognize the N-terminal region of CD20 molecules. We used these antibodies to identify cells that have CD20 molecules with abnormalities in the C-terminal cytoplasmic region. We characterized these mutated CD20 molecules using living primary lymphoma cells.

Correspondence: Dr K Hatake, Department of Clinical Oncology and Hematology, Cancer Institute Hospital, Japanese Foundation for Cancer Research, 3-8-31, Ariake Koto-ku, Tokyo 135-8550, Japan.
E-mail: khatake@jfcr.or.jp
Received 28 October 2010; revised 7 January 2011; accepted 1 February 2011

Materials and methods

Cells, viruses and DNA constructs

The coding region of the *CD20* gene was amplified by reverse transcription PCR (RT-PCR) from RNA extracted from a Burkitt's lymphoma cell line, Raji, and was cloned into a pDON-AI retroviral vector (Takara, Ohtsu, Japan). A series of deletion mutants of CD20 in the C-terminal cytoplasmic region was constructed by inserting stop codons after nucleotides encoding E281, E263, E245, V228 and G210. Retroviruses carrying wild type and deletion mutants of *CD20,* together with mock construct, were produced with the transient retrovirus packaging cell line G3T-hi (Takara) according to the manufacturer's protocol. Packaged retrovirus vectors were then used to infect a myeloma cell line, KMS12PE,[4] with subsequent selection using 500 μg/ml G418.

For the transfection of mutant *CD20* gene, whole coding region of *CD20* complementary DNA (cDNA) prepared by RT-PCR of total RNA isolated from the patient cells was cloned into first cassette of a bicistronic retrovirus vector carrying a green fluorescent protein (Takara). Bicistronic expression of ZsGreen is facilitated by internal ribosomal entry site only when *CD20* mutant gene was translated, enabling the efficient selection of transformed cells.

Generation of monoclonal antibody secreting hybridomas

A synthetic peptide corresponding to residues 23–36 of human CD20 with one additional cysteine at the N-terminus (CMQSGPKPLFRRMSS) was synthesized. The peptide was coupled with keyhole limpet hemocyanin. BALB/c mice were primed with a subcutaneous injection of the keyhole limpet hemocyanin-conjugated synthetic peptide emulsified in Freund's complete adjuvant. Mice were boosted four times at two-week intervals with the same antigen. Mice that developed antibodies as measured by enzyme-linked immunosorbent assay with the immunizing peptide were boosted intravenously with the same peptide 4 days before splenocytes were harvested and fused to mouse myeloma cells. Hybridization and cloning were performed according to standard procedures.[5]

CD20 gene sequencing

Pleural effusion mononuclear cells were obtained by density gradient centrifugation using Ficoll-Hypaque 1.077 (Sigma,

St Louis, MO, USA). The isolated mononuclear cells then underwent negative immunomagnetic selection using a B Cell Isolation Kit II (Miltenyi Biotec, Bergisch Gladbach, Germany) for purifying B-linage cells. Total RNA was prepared using TRIzol reagent according to the instructions of the manufacturer (Invitrogen, Carlsbad, CA, USA) and 1 μg was subjected to reverse transcription under MMLV reverse transcriptase (Takara). To prepare cDNA-containing whole coding region of *CD20*, PCR amplification was performed from 2 μl of cDNA using primers outside of the start and the stop codon: hCD20-5′-FW (5′-GCAGCTAGCATCCAAATCAG-3′) and hCD20-3′-RV (5′-TGGTGCGTATGTGCAGAGTA-3′). To determine the sequence of the *CD20*, we performed cycle sequencing on a 3130 DNA analyzer (Applied Biosystems, Foster City, CA, USA), directly from PCR-purified products, in both directions using a BigDye Terminator Cycle Sequencing Kit v3.1 (Applied Biosystems).

Immunocytochemistry

Cells were stained by rituximab and L26 antibody (DAKO, Carpentaria, CA, USA) sequentially. Briefly, the cells were labeled by incubating in 10 μg/ml of rituximab conjugated with Alexa Fluor 647 (Invitrogen) according to previously described procedure[6] and washed twice with phosphate-buffered saline. Rituximab-labeled cells were swelled by treatment with 75 mM KCl and then were made to adhere onto collagen I-coated cover glass by brief centrifugation. After fixing and permeabilization, the specimens were exposed to L26 antibody. Subsequently, the specimens were washed and were incubated in Alexa488-conjugated goat anti-mouse IgG. Nuclear staining was performed using 5 μg/ml of 4′-6-diamidino-2-phenylindole. The preparations were screened for fluorescence with a confocal microscope (FV1000, OLYMPUS, Tokyo, Japan) using excitation wavelengths of 405, 488 and 633 nm to detect emission by nuclear staining (4′-6-diamidino-2-phenylindole), rituximab or L26 staining, respectively.

Immunohistochemistry

The tissues had been routinely fixed in 10% neutral formalin and embedded in paraffin. L26 antibody and monoclonal antibodies raised against the N-terminal cytoplasmic region of CD20 were used. The sections were deparaffinized and rehydrated in graded alcohol. For heat-induced epitope retrieval, the sections were subjected to Target Retrieval Solution, pH 9 (DAKO) at 97 °C for 40 min. The sections then were brought to an automated stainer (DAKO) by following the vendor's protocol. EnVision Plus (DAKO) and peroxidase detection methods were used.

Rituximab-binding analysis

Rituximab-binding analysis was performed according to our previously developed imaging-based procedure, with some modifications.[6] Briefly, approximately ten thousands cells of purified living lymphoma cells using a Dead cell removal kit (Miltenyi Biotec) were incubated with 10 μg/ml of anti-CD19 mAb labeled with Alexa Fluor 488 (Invitrogen) and rituximab labeled with Alexa Fluor 647 (Invitrogen) for 30 min at 4 °C. The cells were washed with phosphate-buffered saline two times and were then suspended in 4 μl of RPMI1640 medium supplemented with 10% fetal bovine serum and 5 μg/ml of Hoechist 33 342. The cell suspension was pipetted into a well made of silicon, 2.5 mm in diameter and 2 mm in depth, on a piece of cover glass. Images were collected by means of an OLYMPUS PlanApo ×60 oil objective in an OLYMPUS FV-1000 confocal microscope (OLYMPUS). The fluorophore was excited by laser at 405, 488 or 633 nm. The cells were optically sectioned along the *z*-axis, and the images were collected at 640 × 640 pixel resolution in a sequential mode to minimize the crossover between channels. The step size in the *z*-axis was 0.5 μm. For three-dimensional reconstruction, two-dimensional confocal stacks were saved in an Olympus.oib format and three-dimensional images were generated using Fluoview software (OLYMPUS).

Cell sorting and genetic analysis

The cryopreserved B-linage cells of the pleural effusion at relapse were further sorted into two fractions of the cells with high affinity to rituximab (R-high) and those of low (R-low) by using flow cytometry (FACSvantage, Becton Dickinson, Franklin Lakes, NJ, USA). The cells were labeled with rituximab conjugated with AlexaFluor488 (Invitrogen) and anti-CD19-PE (Becton Dickinson), then resuspended in phosphate-buffered saline containing 2 μg/ml of 7-AAD (Sigma) to exclude dead cells. The sorting gate used for 'R-high' was rituximab^{high}/CD19^{+}/7-AAD^{-}, and for 'R-low' was rituximab^{low}/CD19^{+}/7-AAD^{-}. The sorted cells were immediately used for extraction of both genomic DNA and total RNA using QIAamp DNA micro kit and RNeasy micro kit, respectively, (QIAGEN, Hilden, Germany). For amplifying the DNA-containing exon 8 of *CD20* from genomic DNA, PCR was carried out using the forward primer (5′-TTCTGTTTTZGAACATAGTTCTCCCTGTCCA-3′) and the reverse primer (5′-CAGAAAACAGAAATCACTTAAGGAGAG-3′). RT-PCR to amplify the *CD20* cDNA were performed according to the method described above. The PCR and RT-PCR products were used to determine the *CD20* gene sequence by direct sequencing method. In addition, 1 μl of RT-PCR products were cloned into a TA-cloning vector (pCR2.1, Invitrogen) and *CD20* DNA sequences of 16 clones of each RT-PCR product were determined for estimating the ratio of different sequences.

Results

To confirm the epitope of L26, we made a series of constructs of the CD20 molecules with deletion mutations in the C-terminal cytoplasmic domain and introduced them into retrovirus vectors (Figure 1a). KMS12PE cells, in which expression of CD20 is not detected immunohistologically, were then transformed, and we established six kinds of sub-lines with the various C-terminal deletion mutations of CD20. A semi-quantitative RT-PCR analysis using a primer set designed to amplify the *CD20* N-terminal region indicated that no major difference was found in *CD20* messenger RNA (mRNA) expression of the six cell lines (Figure 1b). We carried out immunocytochemical analysis using L26 and fluorescence-labeled rituximab against these six *CD20*-expressing transfectants, along with a mock transfectant and Raji cells as negative and positive controls, respectively. The cells stained by L26 antibody were only those expressing wild type (amino acid 1–297) and DM1 mutant (amino acid 1–281). On the other hand, rituximab could bind to shorter CD20 molecules, such as DM2, DM3 or DM4, as well as to the CD20 molecules recognized by L26 (Figure 1c). These results indicate that L26 antibody recognizes the C-terminal cytoplasm region of CD20 molecules and that its epitope is present in the amino-acid sequence of 264–281. The data suggest that immunohistochemistry using L26 antibody will exhibit a false negative if a deletion or a frame shift occurs upstream of this epitope. In addition, the shortest deletion mutant DM5 that lacked the C-terminal cytoplasmic region was detected by

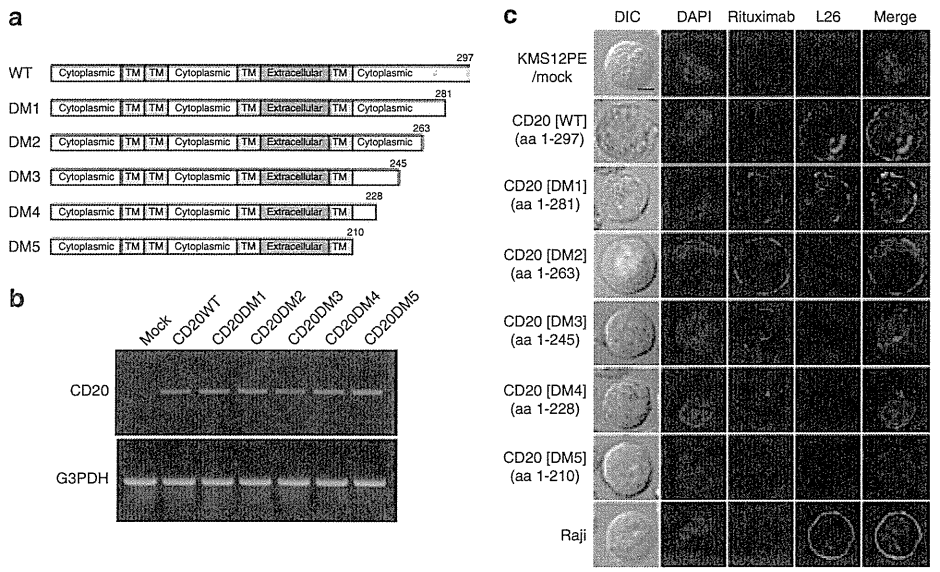

Figure 1 Search for epitopic site of L26 antibody and analysis of the extracellular exposure of CD20 molecules having C-terminal deletion mutation. (**a**) To explore the binding site of the L26 antibody, we constructed various lengths of the CD20 deletion mutant at their C-terminal cytoplasmic domains. TM: transmembrane domain. (**b**) KMS12PE cells retrovirally transduced with C-terminal truncated CD20 showed approximately similar levels of mRNA expression. (**c**) Immunocytochemical studies suggested that L26 recognizes amino-acid sequence between 264 and 281. An objective lens of ×60 was used with a ×10 digital zoom, bar: 5 μm. DAPI, 4′-6-diamidino-2-phenylindole; DIC, differential interference contrast; G3PDH, glyceraldehyde-3-phosphate dehydrogenase; WT, wild type.

neither L26 antibody nor rituximab. Possible reasons might include the low membrane localization of DM5 mutant and/or low stability of the post-translational product. To clarify this, we carried out western blot analysis using total cell lysate of the series of deletion mutants that were tagged by FLAG peptide at the N-terminal region of CD20 constructs. We found that the cellular protein level of the DM5 deletion mutant of CD20 was remarkably lower than that of others, suggesting that low post-translational stability may be the reason for the low antigenicity of DM5 mutant (data not shown).

To detect CD20 in the clinical specimens that acquired rituximab resistance mutations, we developed novel anti-CD20 antibodies and screened them in paraffin sections. We isolated an antibody specific for the CD20 N-terminus and named it CD20N. Using this antibody, we carried out immunohistochemistry conducted on the CD20-negative cases by L26 antibody-based analysis and found several cases with mutations in the C-terminal cytoplasm region. Among them, a cell specimen, a part of which had been cryopreserved as living cells, was included. This was pleural effusion from a patient with relapsed diffuse large cell B-cell lymphoma after complete remission following rituximab containing chemotherapy (rituximab, cyclophosphamide, adriamycin, vincristine and prednisone). This patient did not respond to further treatment with salvage therapies containing rituximab. The results of immunochemical analysis of the fibrin clot of the pleural effusion at relapse, as well as the biopsy of lymph nodes at the first examination, are shown in Figure 2. The lymph node biopsy before rituximab treatment was stained in the same way by both L26 and CD20N antibodies. However, L26 antibody did not stain at the population having mutated CD20 in the pleural effusion. On the other hand, the CD20N antibody stained almost all of the B-cell population. It should be noted that most of the cells were stained at the region of plasma membrane by CD20N antibody.

As a result of DNA sequencing of purified B cells, we found one nucleotide deletion mutation, which caused a frame shift after the amino-acid residue 251, in half of the DNA (Figure 3a). We conducted a binding analysis of rituximab using the viable cells of B-lineage purified from cryopreserved mononuclear cells. Most of these cells were CD19 positive. However, these cells consisted of two kinds of cell populations that were quite different in their affinity for rituximab (Figure 3b). Furthermore, flow cytometry analysis revealed that the fluorescent intensity of fluoro-labeled monoclonal antibody of CD20 decreased to less than one-tenth in about half of the B-cell population (Figure 3c). These results indicate that the C-terminal mutation of the *CD20* gene in this case caused abnormality of extracellular-antigen presentation, even though the protein expression and the cell membrane localization seemed to be normal.

To reveal the genetic mechanisms of the reduced antigenicity to rituximab, we conducted gene-sequencing analysis about both population of cells that differ in affinity to rituximab. The cryopreserved B lymphocytes of the pleural effusion at relapse were sorted into two fractions of cells of high affinity to rituximab (R-high) and those of low (R-low) by using flow cytometry (Figure 4a). Then genomic DNA and total RNA from each fraction were extracted. The results of DNA sequencing of exon 8 of *CD20* in which the mutation was found demonstrated that, surprisingly, both cell populations had both normal and the monobasic deletion mutant *CD20* genes. To determine the proportion of the genes, the PCR-amplified DNA fragments were inserted into a TA-cloning vector and 16 clones from both 'R-high' and 'R-low' fractions were determined the sequence of *CD20*. As a result, the ratio of mutant DNA accounted for approximately half of genomic DNA of both 'R-high' (7 out of 16) and 'R-low' (9 out of 16). On the other hand, the results of sequence analysis about the cDNA revealed that the ratio of mutant mRNA in 'R-low' was remarkably increased (14 out of 16), whereas that of 'R-high' was as the same of the results of genomic DNA (8 out of 16; Figure 4b). We also carried out a sequence analysis about genomic DNA from a slice of paraffin -embedded tissue of lymph node at the first diagnosis of this patient, and found that approximately half of the genomic DNA

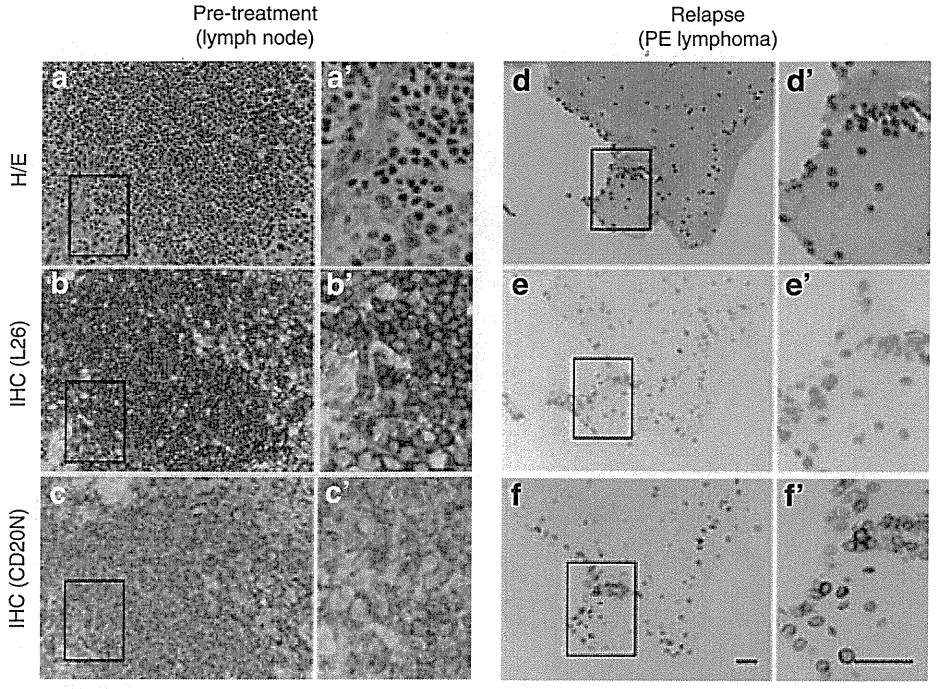

Figure 2 Immunohistochemistry (IHC) was performed on a biopsied specimen of a lymph node at the first examination (**a**, **b** and **c**) and on a fibrin clot from the B-cell population from pleural effusion at the relapse phase (**d**, **e** and **f**). Both L26 and CD20N antibodies uniformly stained the lymphoma cells in the lymph node biopsy specimen (**b** and **c**, respectively). However, L26 did not recognize about half of the B cells derived from pleural effusion (**e**), whereas CD20N stained almost all the cells (**f**). (**a** and **d**) indicates hematoxylin and eosin (H/E) stain. High-magnification images of the region boxed in (**a**–**f**) were shown in (**a'**–**f'**), respectively. An objective lens of × 60 was used, bar: 50 μm. PE lymphoma, lymphoma cell in pleural effusion.

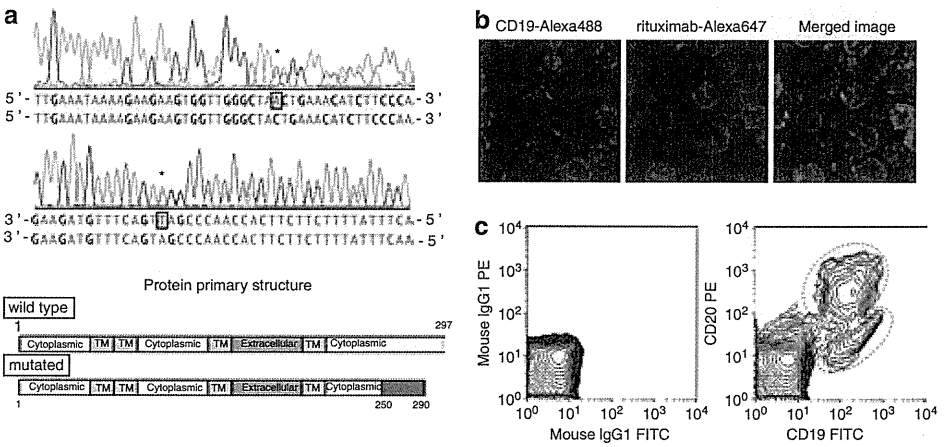

Figure 3 The analysis of primary lymphoma cells derived from pleural effusion of a patient with rituximab-refractory, diffuse large-cell lymphoma. (**a**) A direct sequence analysis of the CD20-coding region revealed that an adenine residue (+478) was deleted in about half of the cDNA. This gene mutation caused a frame shift after the amino-acid sequence of 250 and early denomination. The blue column in the protein schematic charts expresses an abnormal primary structure. *Single nucleotide deletion occurred at this position in approximately half of cDNA. (**b**) Rituximab-binding analysis based on three-dimensional imaging. Magnetically sorted living B-lineage cells were labeled with CD19 (green pseudo-color) and rituximab (red pseudo-color). Although the intensity varied, the CD19 antigen was expressed in most of the cells. Meanwhile, rituximab bound markedly to approximately half of the cells, but the binding to the rest of cells could not be detected. The blue pseudo-color indicates fluorescence of Hoechist22242 nuclear dye. Results shown here are representative of the 19 microscopic fields. (**c**) Flow cytometric analysis of mononuclear cells from the pleural effusion of this patient suggested that there were two populations of different CD20-expressing levels among CD19 positive cells. The mean fluorescence intensities (MFIs) of the higher (blue) and lower (red) CD20-expressing populations were calculated as 486.8 and 30.5, respectively. FITC, fluorescein isothiocyanate.

included the mutant *CD20* gene same as the cells at relapse (8 out of 16; Figure 4c). These results indicated that this patient had already carried the mutation in *CD20* gene, as onset of primary lymphoma, and that a transcriptional imbalance of wild-type *CD20* and mutated *CD20* have occurred by undetermined mechanisms in some cell populations.

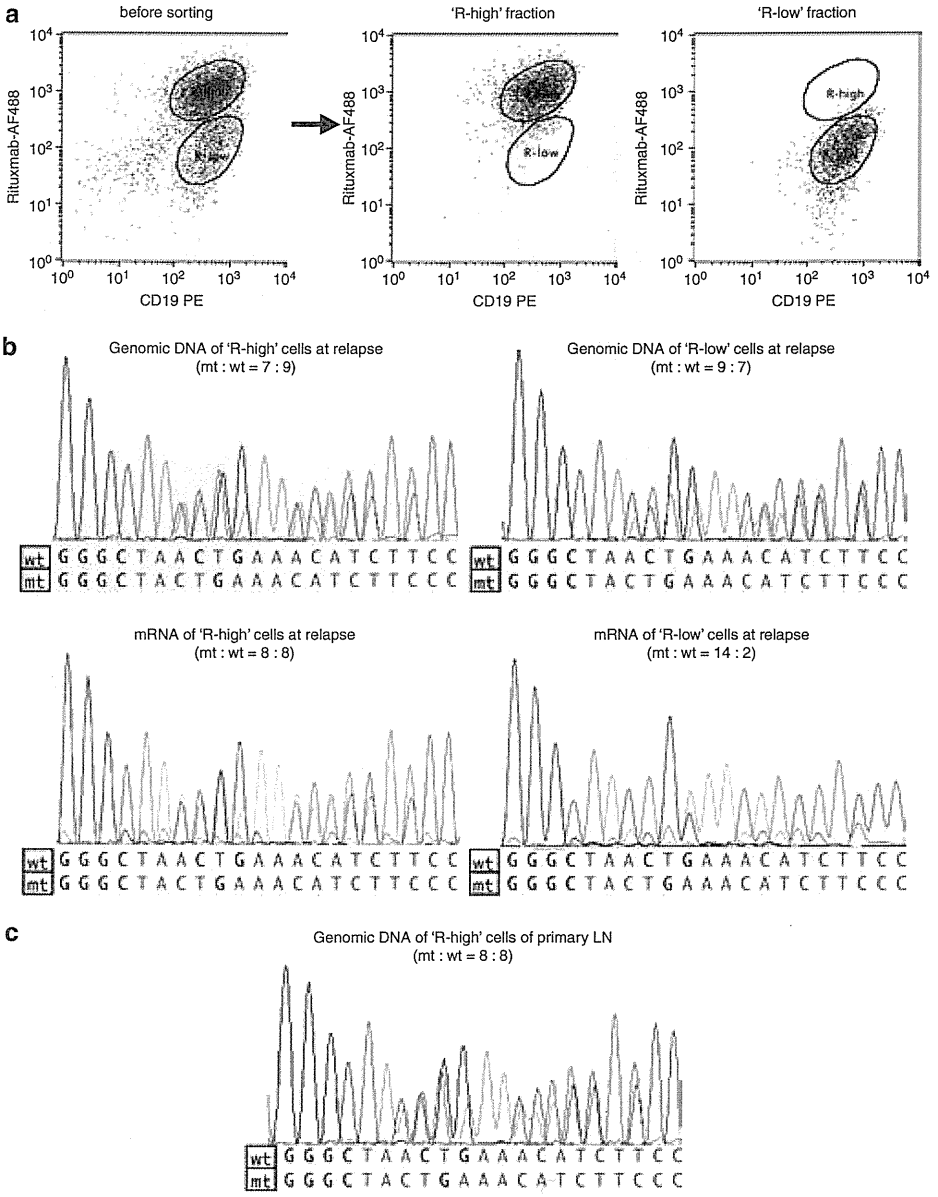

Figure 4 The genetic analysis of patient's lymphoma cells. The cryopreserved B linage cells of the pleural effusion at relapse were further sorted into two fractions of cells with high affinity to rituximab (R-high) and those of low (R-low) by using flow cytometry. (**a**) Dot blot of the cells before and after sorting. (**b**) The results of CD20 sequence analysis of genomic DNA and cDNA of 'R-high' and 'R-low'. The diagrams of direct sequencing of CD20 exon 8 region are shown. The ratio of mutant and wild-type *CD20* genes were determined by the sequencing of 16 clones of RT-PCR products. (**c**) The results of genomic DNA sequence of primary lymphoma.

As CD20 is thought to be present as a tetramer in cells,[7] mutated CD20 may affect also wild-type peptide in the same cell. To verify this possibility, we introduced the *CD20* gene carrying the same mutation as this patient to $CD20^-$ cell line, KMS12PE and $CD20^+$ Daudi using a retrovirus vector, then selected the cells expressing the exogeneous *CD20* by a green fluorescent protein reporter promoted by an internal ribosome entry site (Figure 5a). As the result of evaluating the binding affinity to rituximab by flow cytometry, the exogeneous mutated CD20 exhibited remarkably attenuated antigenicity to rituximab as compared with the wild-type CD20 (Figure 5b). Next, we transformed Daudi cells with the mutant *CD20* to examine the effect on expression of wild-type CD20 molecules. In consideration of turnover of intrinsic CD20, we evaluated binding of rituximab to the transfectants 7 days after virus infection. As shown in Figure 5c, the expression of this mutated CD20 was found to have hardly affected the affinity for rituximab. These results suggested that at least the mutation found in this patient did not exert a dominant negative effect against normal CD20 molecules.

Discussion

Previously, we reported that mutations in the *CD20* gene were found with some frequency in patients treated with rituximab.

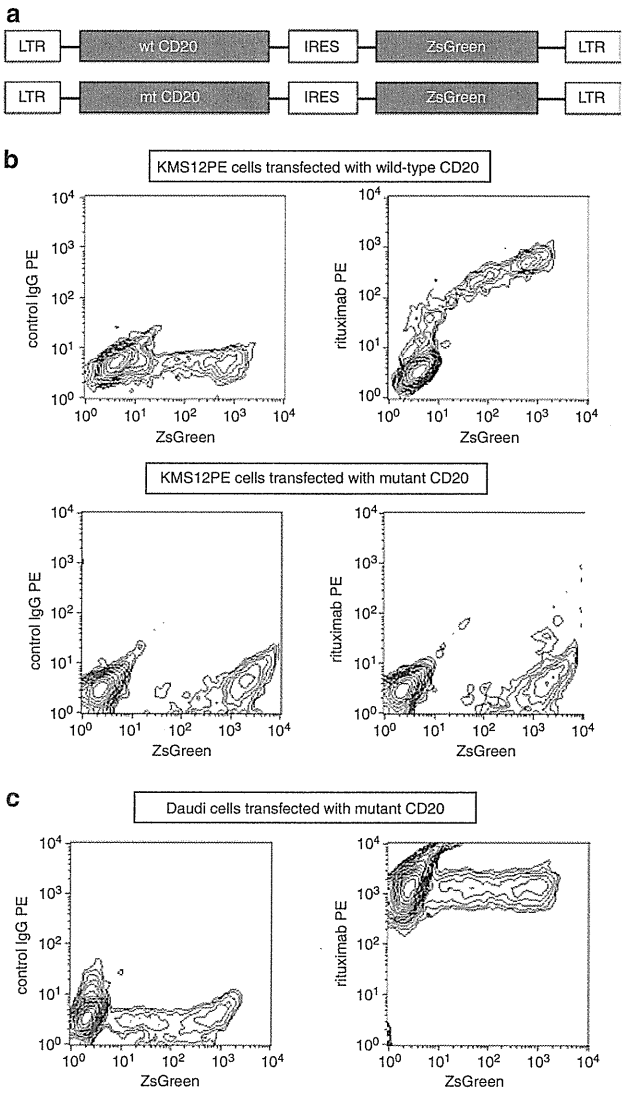

Figure 5 The effect of mutant *CD20* on wild-type *CD20* with respect to rituximab binding. (**a**) The schematic diagram of retrovirus vectors used for transduction of wild-type and mutant *CD20*. (**b**) The transfectants were labeled with PE-conjugated. rituximab and analyzed by flow cytometry at seven days after viral infection. The contour plots of KMS12PE cells transfected with wild-type (upper panel) or mutated *CD20* (lower panel) are shown. (**c**) Daudi cells were transfected with mutated *CD20* and analyzed the rituximab-binding. The mutant *CD20* introduced exogenously hardly affected the binding of rituximab to Daudi cells. IRES, internal ribosome entry site; LTR, long terminal repeat; wt, wild type; mt, mutant.

These cases often have a diagnosis of CD20 negative by immunostaining, based on the commonly used L26 antibody, and are difficult to distinguish from the cases in which protein expression of CD20 is extremely low. So the mutation in the *CD20* gene has been less noticed with regard to resistance to rituximab. In the present study, we roughly identified the epitope of L26, and it became clear that all of the C-terminal-mutated CD20 that we had found earlier lost the epitope for L26, because the epitope was located near the C-terminal of CD20 molecule. To detect CD20 with these mutations comprehensively, we developed monoclonal antibodies that recognize a part of the amino-acid sequence of the N-terminal cytoplasmic region of CD20. One of these antibodies, CD20N, recognized CD20 proteins, including those having a mutation in the paraffin-embedded, formalin-fixed specimen. In this study, we showed that it could be applied to the primary screening of the lymphoma cells that express mutated CD20 by selecting L26-negative and CD20N-positive cells.

To date, there are not many reports that the mutation of the *CD20* gene contributes to resistance to rituximab.[1,8] A part of the reason for this may be that L26 cannot detect most of mutated CD20. In addition, Johnson *et al.*[8] carried out a sequencing screening of exon 5 of the *CD20* gene encompassing the epitope of rituximab. They detected *CD20* mutations involving the rituximab epitope in only 1/264 (0.4%) and 1/15 (6%) of the biopsies taken at diagnosis and relapse, respectively. Similarly, in our previous screening, no mutation was found in the region of exon 5, whereas four cases with mutation (out of 50) were found in the C-terminal cytoplasm region of CD20.[1] In the *CD20* gene, a genetic mutation could be more likely to occur in the C-terminal region compared with around the region of rituximab epitope by uncertain mechanism(s).

By using live cryopreserved cells, derived from a newly identified case with the mutation in the *CD20* gene, we successfully analyzed in detail the phenotype of lymphoma cells having mutated CD20. In this case, a frame shift mutation occurred because of one base nucleotide deletion, resulting in the translation of peptide of another reading frame of 41 amino acids after the amino acid position 250 with a slight early termination. Immunohistochemical analysis using CD20N antibody revealed that the CD20 molecules with C-terminal mutations were indeed expressed in the lymphoma cells, and located at the cell membrane. However, the living cell binding evaluation showed that rituximab could scarcely bind to these cells. These results suggest that the C-terminal region of CD20 undertakes a critical role in presentation of the large loop in which the rituximab-binding site locates.

As a result of genetic analysis for lymphoma cells, it was suggested that this patient had a mutation in the *CD20* gene as onset of primary lymphoma. Because normal and mutated *CD20* gene were almost the same copy numbers and the most of cells in the lymph follicle were stained in L26 at the first diagnosis, it can be considered that the lymphoma cells of this patient had equal number of normal and mutated *CD20* alleles rather than the mixture of the cells having only normal *CD20* allele(s) or only mutant allele(s). And at the relapse, two cell populations of the different affinity for rituximab has arose ('R-high' and 'R-low'), and both had a genome of the same mutation status, however, the expression of the mutated mRNA has been predominant only in 'R-low'. As a result of semi-quantitative RT-PCR analysis revealed that whole *CD20* mRNA expression of 'R-low' slightly decreased as compared with that of 'R-high' (data not shown), the imbalanced mRNA expression in 'R-low' may be due to the suppression of *CD20* mRNA expression from the wild-type allele at the transcription level.

To summarize these data, the primary lymphoma cells of this patient expressed both wild-type and mutated *CD20* equally. As the mutant CD20 in this case was found to have little effect on the antigenicity of wild-type CD20 molecules, these cells were still susceptible to rituximab plus CHOP and the patient has obtained complete remission. However, at the relapse, cells that predominantly expressed the mutant CD20 emerged. This mutant molecule expressed and localized at the plasma membrane, however, the large loop could not be oriented appropriately. So it was considered that rituximab-containing salvage treatments have failed perhaps because affinity for rituximab was not enough.

It was noteworthy that the antibody that recognizes N-terminal region of CD20 has capability to detect the mutated CD20 before start of the salvage therapy. This indicated the possibility that we can predict the existence of lymphoma cells resistant to rituximab before start of therapy. In addition, this information may provide important criterion to judge whether it should switch to the treatment such as using second-generation CD20 antibody that is effective against fewer CD20-expressing cells[9–12] or using antibody for the different target molecule such as CD22.[13,14]

The resistance for a molecular target drug acquired by a mutation in the gene of the target molecule is commonly considered to be irreversible.[15–19] We propose here that detecting a mutation in the gene by screening using antibodies of two kinds of epitope is useful in detection of irreversible resistant mutation for molecular targeted drug including rituximab.

Conflict of interest

The authors declare no conflict of interest.

Acknowledgements

We thank Ms Sayuri Minowa, Ms Harumi Shibata and Ms Mariko Mikuniya for their assistance in specimen preparation. We also thank Dr Dovie Wylie of On-Site English, Inc. (Palo Alto, CA, USA) for English editing assistance.

References

1 Terui Y, Mishima Y, Sugimura N, Kojima K, Sakurai T, Kuniyoshi R *et al.* Identification of CD20 C-terminal deletion mutations associated with loss of CD20 expression in non-Hodgkin's lymphoma. *Clin Cancer Res* 2009; **15**: 2523–2530.
2 Mason DY, Comans-Bitter WM, Cordell JL, Verhoeven MA, van Dongen JJ. Antibody L26 recognizes an intracellular epitope on the B-cell-associated CD20 antigen. *Am J Pathol* 1990; **136**: 1215–1222.
3 Norton AJ, Isaacson PG. Monoclonal antibody L26: an antibody that is reactive with normal and neoplastic B lymphocytes in routinely fixed and paraffin wax embedded tissues. *J Clin Pathol* 1987; **40**: 1405–1412.
4 Hata H, Matsuzaki H, Matsuno F, Sonoki T, Takemoto S, Kuribayashi N *et al.* Establishment of a monoclonal antibody to plasma cells: a comparison with CD38 and PCA-1. *Clin Exp Immunol* 1994; **96**: 370–375.
5 Kohler G, Milstein C. Continuous cultures of fused cells secreting antibody of predefined specificity. *Nature* 1975; **256**: 495–497.
6 Mishima Y, Sugimura N, Matsumoto-Mishima Y, Terui Y, Takeuchi K, Asai S *et al.* An imaging-based rapid evaluation method for complement-dependent cytotoxicity discriminated clinical response to rituximab-containing chemotherapy. *Clin Cancer Res* 2009; **15**: 3624–3632.
7 Polyak MJ, Li H, Shariat N, Deans JP. CD20 homo-oligomers physically associate with the B cell antigen receptor. Dissociation upon receptor engagement and recruitment of phosphoproteins and calmodulin-binding proteins. *J Biol Chem* 2008; **283**: 18545–18552.
8 Johnson NA, Leach S, Woolcock B, deLeeuw RJ, Bashashati A, Sehn LH *et al.* CD20 mutations involving the rituximab epitope are rare in diffuse large B-cell lymphomas and are not a significant cause of R-CHOP failure. *Haematologica* 2009; **94**: 423–427.
9 Pawluczkowycz AW, Beurskens FJ, Beum PV, Lindorfer MA, van de Winkel JG, Parren PW *et al.* Binding of submaximal C1q promotes complement-dependent cytotoxicity (CDC) of B cells opsonized with anti-CD20 mAbs ofatumumab (OFA) or rituximab (RTX): considerably higher levels of CDC are induced by OFA than by RTX. *J Immunol* 2009; **183**: 749–758.
10 Hagenbeek A, Gadeberg O, Johnson P, Pedersen LM, Walewski J, Hellmann A *et al.* First clinical use of ofatumumab, a novel fully human anti-CD20 monoclonal antibody in relapsed or refractory follicular lymphoma: results of a phase 1/2 trial. *Blood* 2008; **111**: 5486–5495.
11 Patz M, Isaeva P, Forcob N, Muller B, Frenzel LP, Wendtner CM *et al.* Comparison of the *in vitro* effects of the anti-CD20 antibodies rituximab and GA101 on chronic lymphocytic leukaemia cells. *Br J Haematol* 2011; **152**: 295–306.
12 Mossner E, Brunker P, Moser S, Puntener U, Schmidt C, Herter S *et al.* Increasing the efficacy of CD20 antibody therapy through the engineering of a new type II anti-CD20 antibody with enhanced direct and immune effector cell-mediated B-cell cytotoxicity. *Blood* 2010; **115**: 4393–4402.
13 Dijoseph JF, Dougher MM, Armellino DC, Evans DY, Damle NK. Therapeutic potential of CD22-specific antibody-targeted chemotherapy using inotuzumab ozogamicin (CMC-544) for the treatment of acute lymphoblastic leukemia. *Leukemia* 2007; **21**: 2240–2245.
14 DiJoseph JF, Goad ME, Dougher MM, Boghaert ER, Kunz A, Hamann PR *et al.* Potent and specific antitumor efficacy of CMC-544, a CD22-targeted immunoconjugate of calicheamicin, against systemically disseminated B-cell lymphoma. *Clin Cancer Res* 2004; **10**: 8620–8629.
15 Pao W, Miller VA, Politi KA, Riely GJ, Somwar R, Zakowski MF *et al.* Acquired resistance of lung adenocarcinomas to gefitinib or

erlotinib is associated with a second mutation in the EGFR kinase domain. *PLoS Med* 2005; **2**: e73.
16 Engelman JA, Janne PA. Mechanisms of acquired resistance to epidermal growth factor receptor tyrosine kinase inhibitors in non-small cell lung cancer. *Clin Cancer Res* 2008; **14**: 2895–2899.
17 Shah NP, Sawyers CL. Mechanisms of resistance to STI571 in Philadelphia chromosome-associated leukemias. *Oncogene* 2003; **22**: 7389–7395.
18 Shah NP, Nicoll JM, Nagar B, Gorre ME, Paquette RL, Kuriyan J *et al*. Multiple BCR-ABL kinase domain mutations confer polyclonal resistance to the tyrosine kinase inhibitor imatinib (STI571) in chronic phase and blast crisis chronic myeloid leukemia. *Cancer Cell* 2002; **2**: 117–125.
19 Wang SE, Narasanna A, Perez-Torres M, Xiang B, Wu FY, Yang S *et al*. HER2 kinase domain mutation results in constitutive phosphorylation and activation of HER2 and EGFR and resistance to EGFR tyrosine kinase inhibitors. *Cancer Cell* 2006; **10**: 25–38.

The Impact of Superior Mediastinal Lymph Node Metastases on Prognosis in Non-small Cell Lung Cancer Located in the Right Middle Lobe

Yukinori Sakao, MD, PhD, Sakae Okumura, MD,* Mun Mingyon, MD, PhD,* Hirofumi Uehara, MD, PhD,* Yuichi Ishikawa, MD, PhD,† and Ken Nakagawa, MD**

Background: We aimed to assess hilar and mediastinal lymph node involvement and its impact on prognosis in patients with right middle lobe lung cancer.

Methods: The records of 170 patients undergoing surgery for right middle lobe non-small cell lung cancer from 1980 to December 2007 were retrospectively examined. There were 45 patients found to have hilar or mediastinal lymph nodes metastases. This subgroup included 31 N2 patients and 14 N1 patients, and included 23 women and 22 men, whose ages ranged from 32 to 83 years (median = 61 years). The status of mediastinal, hilar, and interlobar lymph nodes was assessed according to the seventh edition of the TNM classification for lung cancer. Patient records were examined for age, gender, preoperative nodal status, surgical procedure, metastatic status of lymph nodes (distribution and numbers), tumor size, and histologic features (cell type and differentiation degree). Survival duration was defined as the interval between surgery and death from the tumor or the most recent follow-up.

Results: For N1 cases (n = 14), the most frequent metastatic site was #12m (lymph nodes adjacent to the middle lobe bronchus), which occurred in 11 cases; there was one case with metastases in #11s (lymph nodes between the upper lobe bronchus and bronchus intermedius), and no case with #11i metastases (lymph nodes between the right middle and lower lobe bronchi). The most frequent metastatic mediastinal zone was the subcarinal zone (25/31), and the superior mediastinal zone also had a high incidence of metastases (22/31). Sixteen cases had metastases to both the superior and subcarinal zones, and six cases had metastasis to superior mediastinal zone without subcarinal zone metastasis. When #11s or #11i was involved, eight of nine or five of five, respectively, were N2 cases. Univariate analyses revealed that tumor diameter, cN, status of lymph node metastases, and operative procedure (pneumonectomy) were significant prognostic factors in N2 cases. Regarding status of lymph node metastases, superior mediastinal zone metastases, both superior and inferior (subcarinal) zone metastases, and #11i were significant prognostic factors. Because #11i metastases and superior mediastinal lymph nodes metastases were highly correlated with each other (p = 0.02), two separate models were used in multivariate analyses. Superior mediastinal metastases (p = 0.03) and #11i metastases (p = 0.015) were revealed to be significant independent prognostic factors, whereas multiple-zone metastases only tended toward significance as an adverse prognostic factor (p = 0.054).

Conclusions: Superior mediastinal lymph node metastases and #11i metastases were significant adverse prognostic factors in patients with middle lobe lung cancer, and they were associated with each other.

Key Words: Middle lobe cancer, Superior mediastinal lymph node metastasis, N2, NSCLC.

(*J Thorac Oncol.* 2011;6: 494–499)

The right middle lobe is the smallest lobe in the lung, and lung cancer originating there is much less common than in the other lobes, occurring in 3.8 to 6.7% of all lung cancers.[1–4] The fact that it is less common may be a reason that there are a few reports on the prognostic factors of middle lobe lung cancer.

Lymph drainage from the middle lobe extends to both superior and inferior mediastinal lymph nodes, and previous reports have demonstrated a high incidence of metastases to both the superior and inferior mediastinal zones.[1–6] Nevertheless, there are few articles on the relationships between status of hilar and mediastinal lymph node metastases and patient prognoses.

In this retrospective study, we aimed to clarify prognostic factors in patients with middle lobe lung cancer who underwent surgery. Furthermore, we wanted to determine the association between the status of lymph node metastases and postoperative prognosis.

PATIENTS AND METHODS

This was a retrospective study. Because individual patients were not identified, our institutional review board waived the requirement for obtaining patient consent and approved this study. Between 1980 and December 2007, 170 patients underwent surgical resection at the Cancer Institute

Departments of *Thoracic Surgical Oncology and †Pathology, Japanese Foundation for Cancer Research, Cancer Institute Hospital, Tokyo, Japan.

Disclosure: The authors declare no conflicts of interest.

Address for correspondence: Yukinori Sakao, MD, PhD, Department of Thoracic Surgical Oncology, Japanese Foundation for Cancer Research, Cancer Institute Hospital, 3-10-6, Ariake, Koto-ku, Tokyo 135-8550, Japan. E-mail: yukinori.sakao@jfcr.or.jp

ISSN: 1556-0864/11/0603-0494

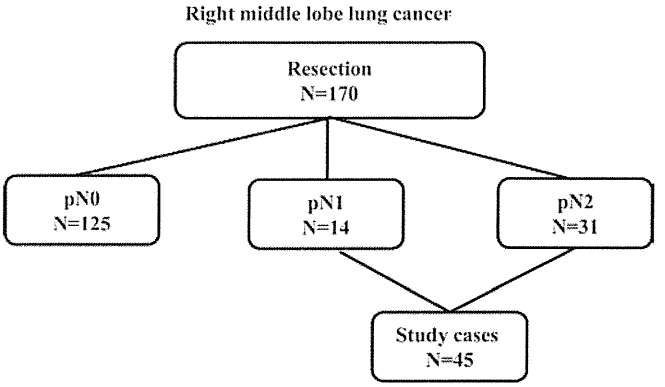

FIGURE 1. Study group subdivisions. Between 1980 and December 2007, 170 patients underwent surgical resections for right middle lobe lung cancer at the Cancer Institute Hospital. There were 14 N1 cases and 31 N2 cases evaluated.

Hospital for primary lung cancer originating in the right middle lobe. Among these patients, 45 were diagnosed with N1 or N2 disease after lung resection and hilar and mediastinal node dissections (Figure 1). The extent of lymph node dissection was not affected by a suspicion of N1 disease. We have routinely performed nearly the same dissection (ND2a).

All the 45 study patients were confirmed for their prognoses. The primary surgical procedure for lymph node dissection, such as hilar and mediastinal nodal dissection, was established in Japan in the late 1970s. In our institute, the extent of lymph node dissection conducted recently is nearly the same as that during the 1980s. Some cases had sampling due to disorders such as cardiac or pulmonary, and these cases were excluded from this study. The resected lymph nodes were separated according to the map[7] in the operating room by the surgeons. Station 10 nodes dissected in middle lobe cancer were adjacent to the inferior parts of the main bronchus, and these nodes were included in the subcarinal zone according to the new TNM. [7] The other station 10 nodes, which were adjacent to the upper parts of the main bronchus, were not routinely dissected, and this area is difficult to dissect without an upper lobectomy.

This subgroup included 31 N2 patients and 14 N1 patients, and included 23 women and 22 men, whose ages ranged from 32 to 83 years (median = 61 years, Table 1). For all patients, preoperative staging was performed using chest computed tomography (CT), abdominal CT or ultrasonography, brain CT or magnetic resonance imaging, and bone scans. Clinical mediastinal and hilar lymph node status was assessed as positive if the chest CT showed that the short axis of a node was more than 1.0 cm. CT scans have been used for evaluating lung cancer staging in our institute since 1980. Of course, CT imaging quality is different when comparing that in the 1980s with that in the 2000s. Nevertheless, this study focused on pathological N status of middle lobe lung cancer, and the quality of pathological examinations was nearly the same during the study period. We excluded those patients who had induction therapy because it seemed to be difficult to evaluate their pathological node status.

TABLE 1. Patient Characteristics

Age (yr)	32–83, median: 61
Gender (male/female)	22/23
c-N	
N0/N1/N2	23/14/8
c-T	
T1/T2/T3/T4	17/24/3/1
p-N	
N1/N2	14/31
Histologic type	
Adenocarcinoma/others	35/10
Well-differentiated/others	10/35
Surgical procedure	
Lobectomy/bilobectomy/pneumonectomy	21/14/10

Bulky N2 (shortest mediastinal lymph node diameter >2 cm) patients have not been candidates for surgery in our institute. Although mediastinoscopy, 18F-fluorodeoxyglucose positron emission tomography, or endobronchial ultrasound with transbronchial needle aspiration was applied to some patients in this series, they were not used for preoperative staging. Follow-up periods ranged from 2 to 302 months (median follow-up for living patients was 86 months).

The status of mediastinal, hilar, or interlobar nodes was assessed according to the seventh edition of the TNM classification for lung cancer.[7] Mediastinal nodes were classified into the following three zones: superior, subcarinal, and inferior. N1 nodes were classified into two zones as hilar or interlobar, and peripheral. The interlobar zone was divided into three subgroups as follows: #12m, lymph nodes adjacent to the middle lobe bronchus; #11s, lymph nodes between the upper lobe bronchus and bronchus intermedius; and #11i, lymph nodes between the right middle and lower lobe bronchi. When a case had mediastinal nodal involvement of two or more zones, it was classified with multiple-zone metastases.

Patient characteristics are summarized in Table 1. Patient records were examined for age, gender, preoperative nodal status, surgical procedure, metastatic status of lymph nodes (distribution and numbers), tumor size, and histologic features (cell type and degree of differentiation).

Statistical Analysis

Survival duration was defined as the interval between surgery and death from the tumor, or the most recent follow-up. Survival rates were calculated using the Kaplan-Meier method. Univariate analyses were performed using the log-rank test, χ^2 test, and logistic regression. Multivariate analyses were performed for variables with p values less than 0.1 by univariate analysis, using the logistic regression test in StatView J 5.0 (SAS Institute Inc., Cary, NC). A p value less than 0.05 was considered significant.

RESULTS

Status of Lymph Node Metastases

In N1 cases (n = 14), the most frequent metastatic site was #12m, occurring in 11 cases, and there was one case with metastases in #11s and 0 cases with #11i metastases (Figure 2).

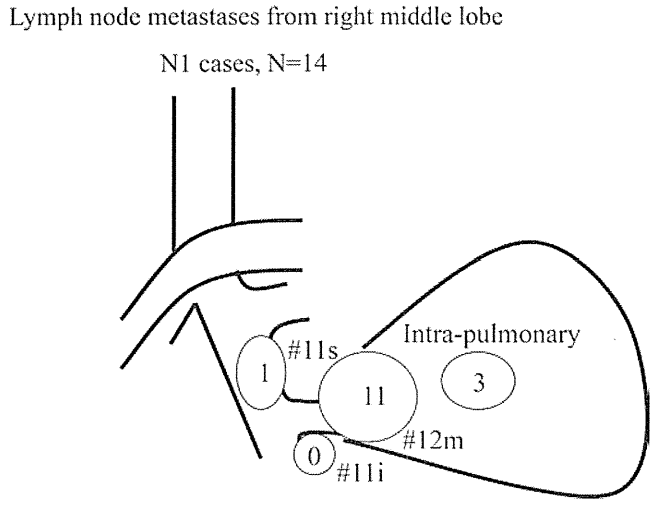

FIGURE 2. Distribution of metastatic nodes in N1 cases.

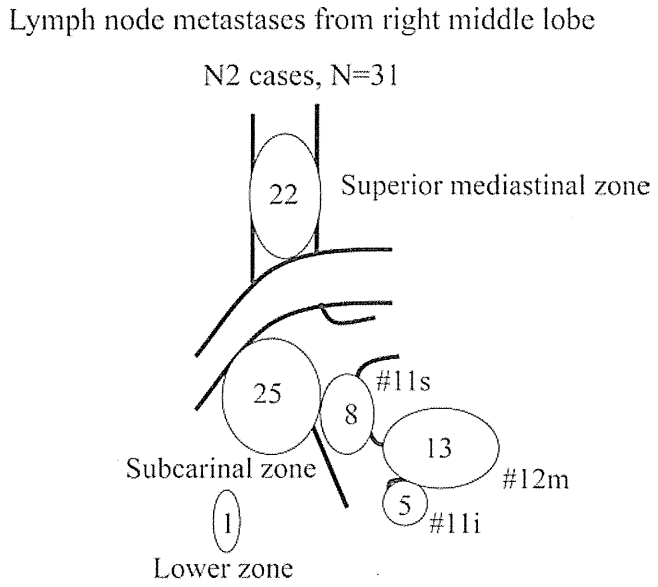

FIGURE 3. Distribution of metastatic nodes in N2 cases.

The most frequent metastatic mediastinal zone was the subcarinal zone (25/31 N2 cases). The superior zone also had a high incidence of metastases (22/31 cases). There were 16 cases with metastases in both the superior and subcarinal zones; nine cases were metastasized to the subcarinal zone without the superior mediastinal zone metastasis, and six cases were metastasized to superior the mediastinal zone without the subcarinal zone metastasis (Figure 3). When #11s was involved, eight of nine cases were N2, and when #11i was involved, all five cases were N2 (Figures 4 and 5).

Survival Rates for Patients with Nodal Involvement

The postoperative 5-year survival rate for patients with N1 was 62% and with N2 was 20% ($p = 0.02$). The postoperative 5-year survival rate was 83% for 125 N0 patients. The prognoses for N0 patients with right middle lobe cancers were not different from those of N0 patients with other involved lobes.

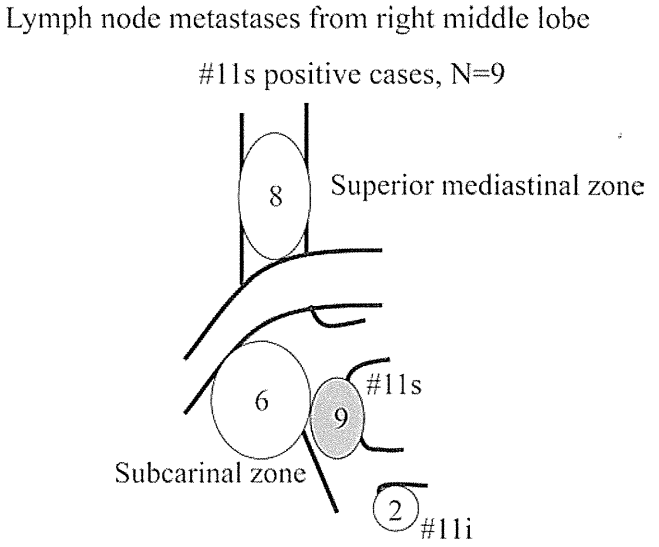

FIGURE 4. Association of #11s metastases with mediastinal zone metastases.

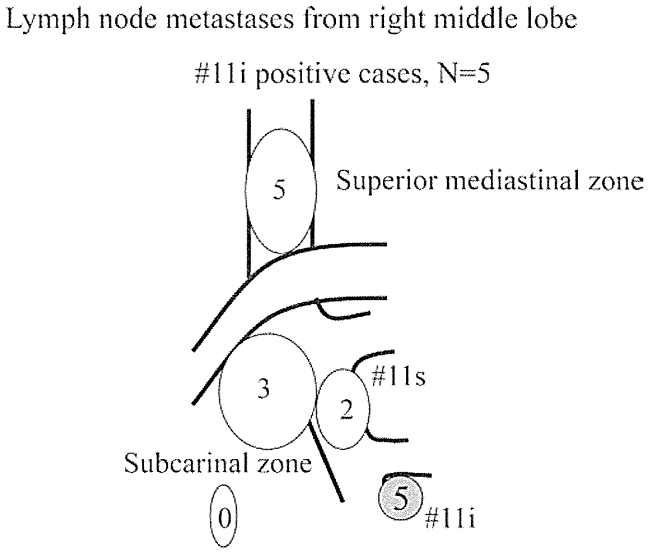

FIGURE 5. Association of #11i metastases with mediastinal zone metastases.

Prognostic Factors for N2 in the Right Middle Lobe

Univariate analyses using the variables listed in Table 2 showed that diameter, cN1–2/cN0, status of lymph node metastases, and operative procedure (pneumonectomy) were significant prognostic factors. Nevertheless, there was no difference in prognoses between lobectomy and bilobectomy. Regarding specific prognostic lymph node metastases, superior mediastinal zone metastases, both superior and subcarinal and interlobar #11i metastases were significant prognostic factors. Inferior mediastinal zone metastases, and #12m and

TABLE 2. Prognostic Factors for Patients with N2: Univariate Analysis

Variables	Cases	5-yr Survival (%)	*p*
Gender			
Male/female	14/17	17.8/22.0	0.95
Age			
<70 yr/70 yr or older	22/9	21.7/16.0	0.37
Diameter (14–65 mm, mean: 35 mm)			
<35 mm/35 mm or larger	16/15	36.5/6.8	0.02
cN			
cN1–2/cN0	15/16	8.0/33.7	0.042
cN0–1/cN2	23/8	23.3/12.5	0.24
Adenocarcinoma/others	26/5	25.2/0	0.1
Well differentiated/others	6/25	16.7/21.5	0.81
Pleural involvement yes/no	15/16	21.8/17.3	0.57
Status of lymph node metastases			
Superior mediastinal zone yes/no	22/9	6.4/50.8	0.005
Inferior mediastinal zone yes/no	25/6	21.4/16.7	0.61
#12m yes/no	13/18	24.7/18.3	0.92
#11s yes/no	8/23	14.3/21.9	0.14
#11i yes/no	5/26	0/23.6	0.02
Both superior and inferior zones			
Multiple zones/single zone	16/15	0/36.4	0.01
Operative procedure			
Pneumonectomy vs. others	7/24	0/25.8	0.009
Lobectomy vs. bilobectomy	16/8	23.6/29.2	0.61
Period			
Before 1995 vs. from and after 1995	15/16	13.3/28.4	0.28

#12m, lymph nodes adjacent to middle lobe bronchus; #11s, lymph nodes between the upper lobe bronchus and bronchus intermedius; #11i, lymph nodes between the right middle and lower lobe bronchi.

TABLE 3. Prognostic Factors for Patients with N2: Multivariate Analysis

Variables	Odds Ratio	95% CI	*p*
Model 1			
Diameter	1.04	0.99–1.08	0.054
cN			
cN1–2/cN0	1.87	0.71–4.95	0.21
Status of lymph node metastases			
Superior mediastinal zone	5.08	1.20–21.8	0.03
Multiple zones	1.42	0.51–3.96	0.50
Operative procedure			
Pneumonectomy	1.13	0.30–4.34	0.88
Model 2			
Diameter	1.03	0.99–1.06	0.17
cN			
cN1–2/cN0	1.38	0.54–3.52	0.51
Status of lymph node metastases			
#11i	4.80	1.34–17.0	0.015
Multiple zones	2.80	0.98–7.96	0.054
Operative procedure			
Pneumonectomy	2.32	0.62–10.0	0.20

#11i, lymph nodes between the right middle and lower lobe bronchi.

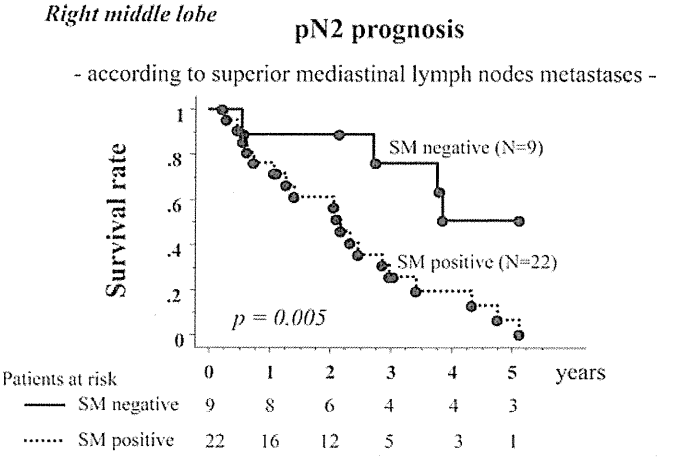

FIGURE 6. Postoperative survival according to superior mediastinal nodal involvement.

#11s metastases were not significant. There was no difference in prognoses between the patients before 1995 and patients from 1996 and after (5-year survivals of 13.3% and 28.4%; $p = 0.28$).

Significant variables by univariate analyses were analyzed by multivariate analyses (Table 3, models 1 and 2). Because #11i metastases and superior mediastinal lymph nodes metastases were highly correlated with each other ($p = 0.02$), two separate models were used for multivariate analyses. In model 1, superior mediastinal metastases were revealed to be a significant independent prognostic factor ($p = 0.03$). In model 2, #11i metastases were revealed to be a significant independent prognostic factor ($p = 0.015$), whereas multiple zone metastases only tended toward significance as an adverse prognostic factor ($p = 0.054$).

Survival Rate According to Prognostic N2 Factors

N2 patients were categorized according to whether they had significant prognostic factors determined from multivariate analyses, including superior mediastinal lymph nodes metastases, #11i metastases, or multiple mediastinal metastatic zones.

The 5-year survival rate was 50.8% in patients without superior mediastinal lymph nodes metastases, whereas it was 6.4% in patients with superior mediastinal lymph node metastases ($p = 0.005$, Figure 6). The 5-year survival rate was 23.6% in patients without #11i lymph node metastases, whereas there were no long-term survivors (dead within 3 years) in patients with #11i lymph node metastases ($p = 0.008$, Figure 7). Furthermore, the 3-year and 5-year survival rates were 58.2% and 36.4% in patients with single-zone mediastinal lymph node metastases, whereas they were 29.6% and 0% in patients with multiple-zone mediastinal lymph node metastases ($p = 0.01$), respectively. Nevertheless, by multivariate analysis, superior mediastinal lymph

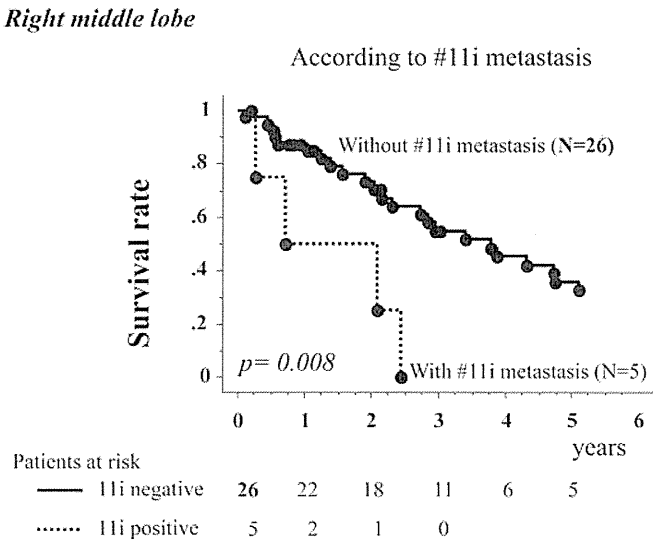

FIGURE 7. Postoperative survival according to #11i nodal involvement.

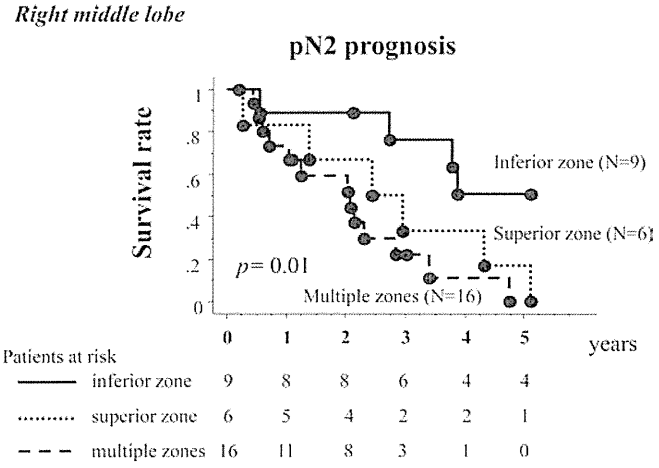

FIGURE 8. Postoperative survival: comparison of superior mediastinal nodal involvement with multiple-zone metastases.

node metastases were revealed to be a stronger prognostic factor than multiple metastatic zones (Figure 8).

DISCUSSION

There have been many reports on the prognostic impact of metastasis to specific mediastinal zones, especially lung cancer in the upper or lower lobes. For patients with lung cancer with tumor originating in the upper lobe or division, the frequency of subcarinal lymph node metastases has been reported to range from 3 to 5%, with the 5-year survival rates ranging from 9 to 18%.[8–10] The frequency of superior mediastinal lymph node metastases has been reported to range from 4 to 5%, with 5-year survival rates ranging from 0 to 19%.[10,11] This low-frequency mediastinal lymph node involvement was highly associated with multilevel N2, and therefore, the outcomes were poor.[10,12,13] In this study, the frequency of metastases was similar for the subcarinal and superior mediastinal zones, and the incidences in N2 patients were 80.6% and 71.0%, respectively. Thus, both superior and inferior mediastinal zones were found to be major metastatic sites, and these results are compatible with previous reports.[14]

We have revealed that metastases to the superior mediastinal lymph nodes are an important independent prognostic factor in patients with N2 middle lobe cancer. This is similar to what is seen in lower lobe cancer. Nevertheless, the incidence of skip metastasis to the superior mediastinum is very different between cancer in the middle lobe and in the lower lobe. The incidence in this study was 20% for N2 and has been reported to range from 3 to 4.5% in N2 right lower lobe cancer.[10–12] Furthermore, there was a significant difference in the 5-year survival rates for superior mediastinal involvement and inferior mediastinal involvement (6.5% and 50.8%, respectively), even for single-zone N2. When superior mediastinal lymph nodes were involved, the prognosis was almost the same as for multilevel N2 patients with middle lobe cancer.

The most frequent metastatic hilar lymph node was #12m, and most #11s and #11i metastases were found in N2 patients. In other words, metastases found in #11s or #11i indicate N2 disease (#11s: 8/9 and #11i: 5/5). Surprisingly, interlobar (lower lobe: #11i) lymph node involvement was an important adverse prognostic factor, even in N2 patients. This may be explained by the fact that there was an association between #11i metastases and superior mediastinal nodal involvement. Metastasis in #11i may be understood to be a result of mediastinal nodal involvement. That is, #11i metastasis is retrograde because of disturbed antegrade lymph drainage to the superior mediastinum from mediastinal metastases. Unfortunately, we could not find any previous reports regarding this correlation between #11i and superior mediastinal node involvement. Further investigation is needed to prove the hypothesis that #11i metastases result from superior mediastinal lymph node metastases.

In conclusion, superior mediastinal lymph node metastases and #11i metastases were significant adverse prognostic factors in patients with middle lobe lung cancer, and they were associated with each other. Furthermore, in patients with middle lobe lung cancer, #11i metastases may result from mediastinal metastases, and the impact on prognosis must be different from that of patients with cancer in other lobes.

Limitations of this study include its retrospective nature, including cases from the 1980s, a small sample number, and that routine adjuvant chemotherapy for N2 patients was started in 2006. Therefore, in this study, it was difficult to evaluate the effects on prognosis with respect to adjuvant chemotherapy.

REFERENCES

1. Vincent RG, Takita H, Lane WW, et al. Surgical therapy of lung cancer. *J Thorac Cardiovasc Surg* 1976;71:581–591.
2. Freise G, Gabler A, Liebig S. Bronchial carcinoma and long-term survival. Retrospective study of 433 patients who underwent resection. *Thorax* 1978;33:228–234.